Upper Cretaceous chalk facies and depositional history recorded in the Mona-1 core, Mona Ridge, Danish North Sea

Kresten Anderskouv and Finn Surlyk

Citation of the name of this series
It is recommended that the name of this series is cited in full, viz. *Geological Survey of Denmark and Greenland Bulletin*.
If abbreviation of this volume is necessary, the following form is suggested: *Geol. Surv. Den. Green. Bull.* 25, 60 pp.

Available from
      Geological Survey of Denmark and Greenland (GEUS)
      Øster Voldgade 10, DK-1350 Copenhagen K, Denmark
      Phone: +45 38 14 20 00, fax: +45 38 14 20 50, e-mail: geus@geus.dk

or at   *www.geus.dk/publications/bull*

Contents

Abstract

Anderskouv, K. & Surlyk, F. 2011: Upper Cretaceous chalk facies and depositional history recorded in the Mona-1 core, Mona Ridge, Danish North Sea. *Geological Survey of Denmark and Greenland Bulletin* 25, 60 pp.

The 331 m long core from the Mona-1 well in the Danish North Sea spans almost the entire Upper Cretaceous Chalk Group but only about 10% of Late Cretaceous time is represented. The succession comprises 14 facies representing pelagic deposition, turbidity flow, and mass-transport processes, including mudflow, debris flow, and slumping. Pelagic deposits vary mainly in terms of the concentration of siliciclastic material, the trace-fossil assemblage, and the presence or absence of primary sedimentary structures. Pelagic sedimentation was probably punctuated by the deposition of thin turbidites, and the resultant deposits were thoroughly bioturbated if deposited during normal oxygenation at the sea floor. Periodic benthic dysoxia resulted in the preservation of primary structures, as represented by laminated chalk which consists of thin pelagic laminae alternating with thin turbidites. In addition to the thin turbidites in the laminated chalk, four different turbidite facies are interpreted as representing high- to low-energy flows. Clast-supported chalk conglomerates have previously not been differentiated from other turbidites, but are here interpreted to be directly related to the down-slope evolution of debris flows. Debris flows are represented by matrix-supported conglomerates, which form one of the most common facies in the succession. High-concentration, gravity-driven suspension flows passed into dilute visco-plastic flows during the final stages of deposition and resulted in the deposition of structureless chalks. Limited shear deformation produced distinct quasi-facies from which the precursor facies can be deduced, whereas intense or continued shear deformation produced a shear-banded quasi-facies from which the precursor facies cannot be deduced in all cases. A series of major slump packages (14–18 in total) are interpreted, forming over 40% of the succession; debrites appear to be the most common precursor facies involved in slumping.

The vertical succession of facies records an earliest Cenomanian facies shift from dominantly siliciclastic to chalk deposition. The Cenomanian – late Campanian period was dominated by erosion or sediment by-pass with minor associated mass-transport deposits preserved. Basin filling by pelagites and turbidites prevailed in the late Campanian, whereas Maastrichtian pelagic deposition was interrupted by increasingly frequent and voluminous mass-transport events.

Authors' address
Department of Geography and Geology, University of Copenhagen, Øster Voldgade 10, DK-1350 Copenhagen K, Denmark.
E-mail: *ka@geo.ku.dk, finns@geo.ku.dk*

Introduction

The Upper Cretaceous Chalk Group has long been the subject of research concentrating on stratigraphy, palaeontology and geochemistry. Few studies have addressed the physical processes of deposition in detail, with some notable exceptions (e.g. Voigt 1962, 1977; Voigt & Häntzschel 1964; Steinich 1967, 1972; Kennedy & Juignet 1974; Kennedy & Garrison 1975; Gale 1980; Hardman & Kennedy 1980; Noe-Nygaard & Surlyk 1985; Quine & Bosence 1991; Scholle et al. 1998; Damholt & Surlyk 2004; Anderskouv et al. 2007), and almost no empirical data on the depositional processes of chalk ooze exist. As a result, the literature contains few examples of depositional models for chalk and none of those published have been demonstrated to be successfully predictive, with respect to identifying the occurrence of a particular facies based on the known occurrence of other facies. Vertical successions of chalk facies in the Chalk Group of the North Sea have been considered non-ordered, unlike the commonly systematic and predictable stacking patterns of deep-water sili-ciclastic successions (e.g. Surlyk et al. 2003). Although this is mainly due to the line-sourced nature of most carbonate redeposition systems and the fact that most redeposition processes may be initiated at any depth on the slope (e.g. Mullins & Cook 1986), it probably also reflects a relatively limited understanding of the lateral associations and gradations between processes and facies in the Chalk Sea.

Descriptive classification schemes for chalk facies or lithologies have been introduced (Hancock 1975; Siemers et al. 1994; Crabtree et al. 1996). The understanding of depositional systems can be used to predict the distribution of facies or lithologies, a task that is interpretive by nature. Objective description is necessary to document and communicate an interpretation, but it has no predictive power in itself. A variety of interpretive facies and conceptual depositional models for the North Sea Chalk Group have also been proposed (Nygaard et al. 1983; Brewster et al. 1986; Kennedy 1987a, b; Nielsen et al. 1990; Sikora et al. 1998; Bramwell et al. 1999). Such models may prove predictive when based on a solid foundation of empirical data and/or numerous well-documented cases. The purpose of the present paper is to contribute to such a foundation by presenting a detailed study of a long and varied succession. The analysis builds upon all the papers cited
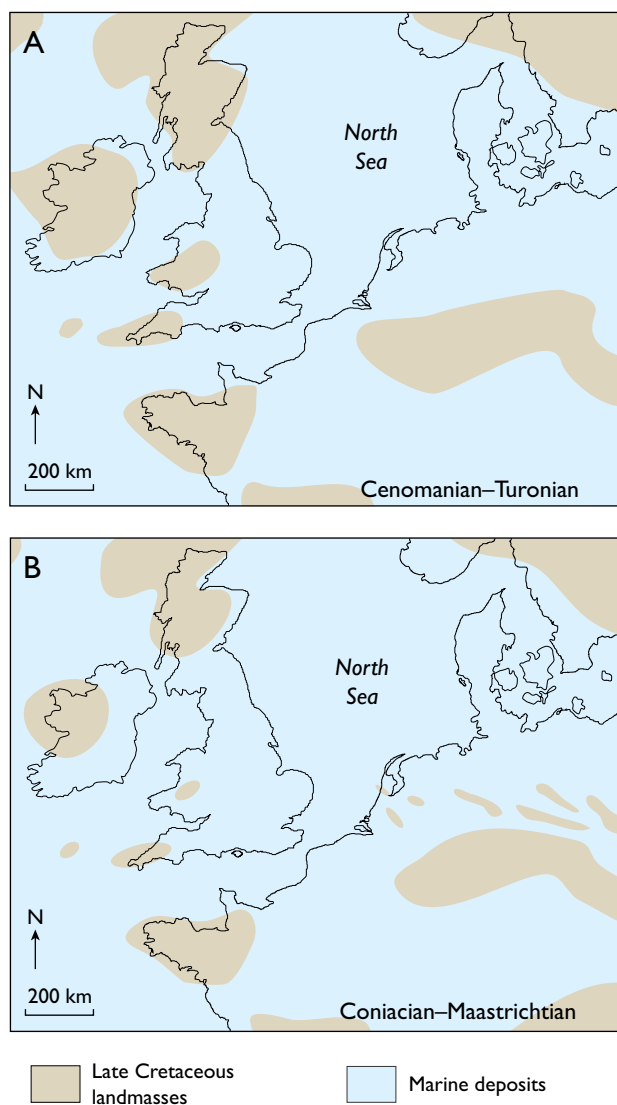
Fig. 1. Palaeogeography of North-West Europe during the Cenomanian–Turonian (**A**), and the Coniacian–Maastrichtian (**B**). Modified from Ziegler (1990).

Facing page:
Fig. 2. **A**: Main structural elements in the North Sea Central Graben. Modified from Surlyk et al. (2003). **DK**: Denmark. **Ger.**: Germany. **Neth.**: Netherlands. **UK**: United Kingdom. **B**: Structural elements and Chalk Group isochore contours in metres in the Mona Ridge area. The shaded area, where the Chalk Group is less than 600 m thick, broadly defines the position of the Mona Ridge. The dashed line indicates the location of the seismic line in Fig. 3. Modified from Britze et al. (1995).
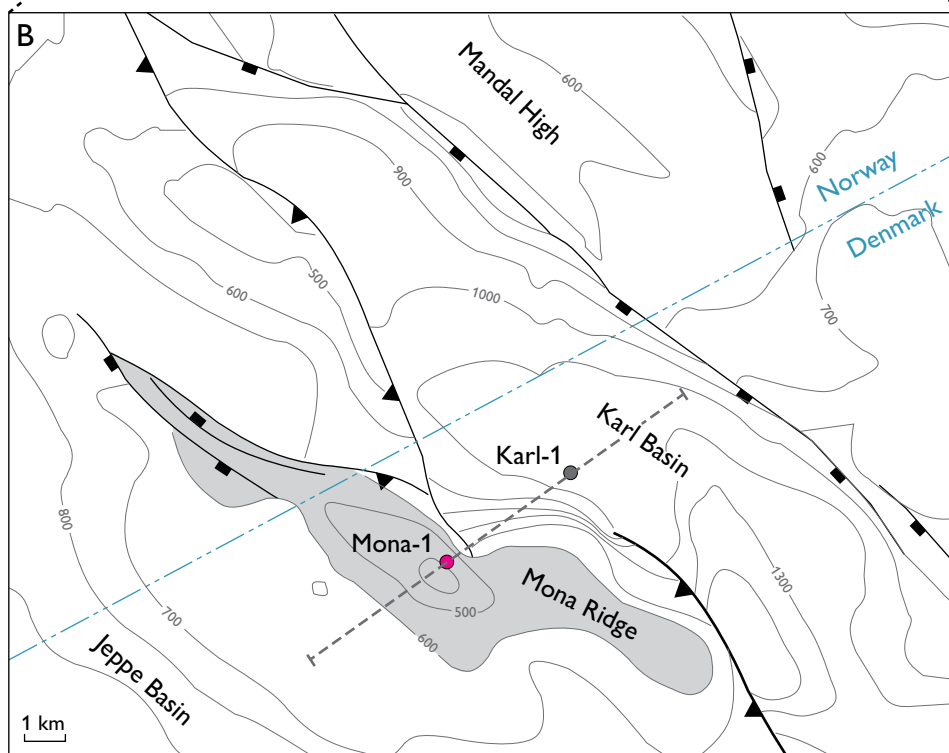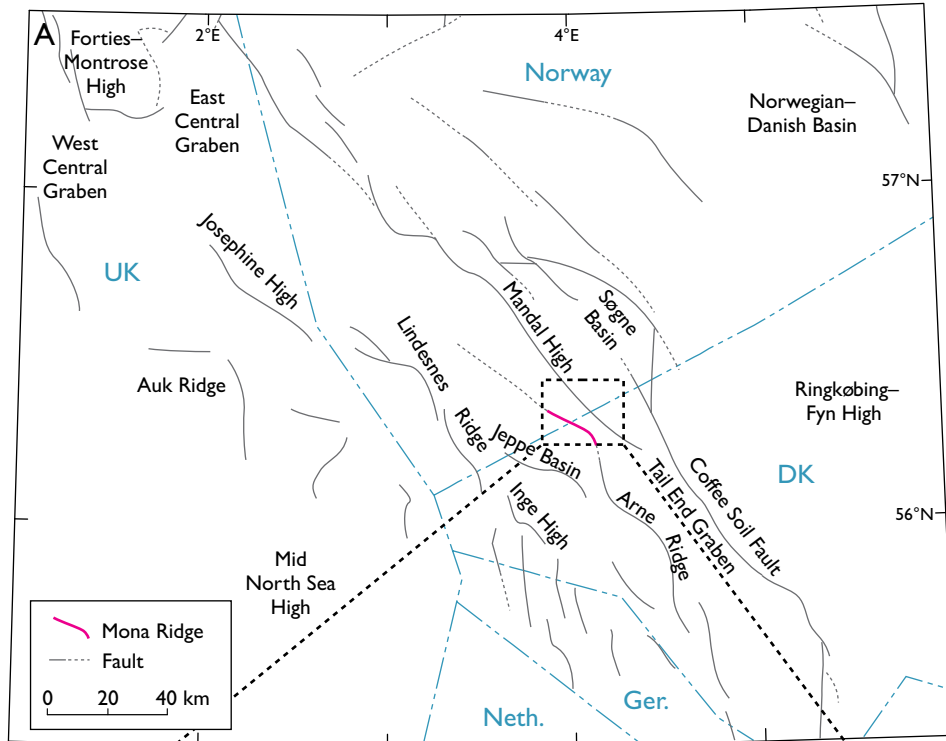
above although the facies descriptions do not rely on a classification scheme and interpretations do not follow a specific depositional model. Nor is the applied facies subdivision presumed to constitute a universally employable facies scheme. The Mona-1 core is ideal for the purpose of the study as it covers a 303 m long chalk succession ranging from the base Upper Cretaceous almost to the Cretaceous–Tertiary boundary. A wide range of chalk facies are represented in the succession, which thus provides an excellent opportunity for analysing the vertical development of chalk facies in the Upper Cretaceous part of the Chalk Group in the North Sea. The aim of this study is to present detailed descriptions and interpretations of the chalk facies present, and to discuss facies associations and the general Late Cretaceous depositional history in the Mona Ridge area.

Setting and stratigraphy

During the Late Cretaceous, much of North-West Europe was covered by an extensive epeiric sea that was characterised by low terrigenous input and deposition of chalk (Håkansson *et al.* 1974; Hancock 1976; Surlyk 1997; Surlyk *et al.* 2003). The central North Sea area constituted a relatively deep part of the Chalk Sea, flanked to the east by the wide pelagic carbonate ramp and basin of the Danish Basin, the siliciclastic-dominated seas towards the north, the shallower seas around the present British Isles to the west, and the Paris Basin to the south (Fig. 1). The Central Graben is a generally NNW-trending intracratonic basin in the North Sea, delimited by the Coffee Soil Fault to the east and the Mid North Sea High to the west. It was formed by Permian and Triassic rifting, Middle Jurassic thermal uplift and Late Jurassic rifting along N- to NE-trending normal faults (e.g. Zanella & Coward 2003). Thermal subsidence characterised the Late Cretaceous, punctuated by inversion pulses (Cartwright 1989; Vejbæk & Andersen 2002). The Mona Ridge is an elongate NW–SE-trending structural high in the northernmost part of the Danish North Sea near the eastern limit of block
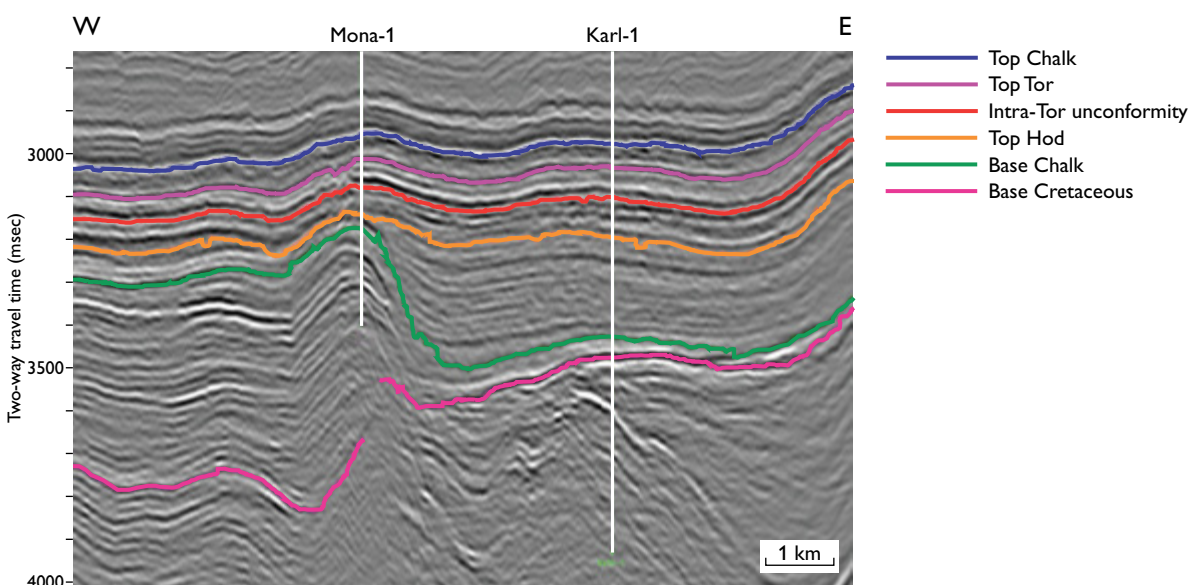
Fig. 3. Seismic section from the eastern part of the Jeppe Basin (left) to the western margin of the Mandal High (right); for location of seismic line, see Fig. 2. Interpretation courtesy of F.C. Jakobsen (GEUS).

Stratigraphy

System	Series	Stage			Central North Sea	
Palaeogene	Paleocene	Danian			Ekofisk Formation	Roga-land Group
Cretaceous	Upper	Maastrichtian	upper		Tor Formation	Chalk Group
			l			
		Campanian	upper		Hod Formation	
			middle			
			lower			
		Santonian	u			
			m			
			l			
		Coniacian	u			
			m			
			l			
		Turonian	u			
			m			
			l		Blodøks Formation	
		Cenomanian	u		Hidra Formation	
			m			
			lower			
	Lower	Albian	upper			Cromer Knoll Group

Fig. 4. Lithostratigraphic subdivision of the Chalk Group in the North Sea. Modified from Surlyk et al. (2003). **l**: lower. **m**: middle. **u**: upper.

Depth (m)	Depth (ft)	Series	Stage	Nannoplankton Zone
3150	10350	Upper Cretaceous	upper Maastrichtian	UC20
3160				
3170	10400			
3180	10450			
3190				
3200	10500			
3210	10550			
3220				
3230	10600			
3240				
3250	10650			
3260	10700			
3270				
3280	10750			UC19
3290	10800			
3300				
3310	10850			
3320	10900			
3330				
3340	10950		lower Maastrichtian	UC18
3350	11000			
3360				
3370	11050			
3380	11100			
3390			upper Campanian	UC16
3400	11150			
3410	11200			
3420			Cenoman.	UC11 ***
3430	11250			UC10 **
3440				UC3*
3450	11300	L.Cr.	Alb.	BC27

Fig. 5. Biostratigraphy of the Mona-1 core based on calcareous nannofossils. Modified from Bailey et al. (1999). Grey parts denote lack of nannofossil data due to gaps between samples or poor preservation. **Alb.**: Albian. **Cenoman.**: Cenomanian. **L.**: Lower. **Cr.**: Cretaceous.

*   UC3 or older
**   middle–upper Coniacian
*** upper Coniacian – lower Santonian

21 (Fig. 2). It is flanked to the SW by the wide, NW–SE-trending Jeppe Basin and to the NE by the narrow and deep Karl Basin (Fig. 3). The Karl Basin is delimited by the Mona Ridge and the Mandal High further to the NE. The Mona-1 well is situated just east of the crest of the Mona Ridge adjacent to the Karl Basin.

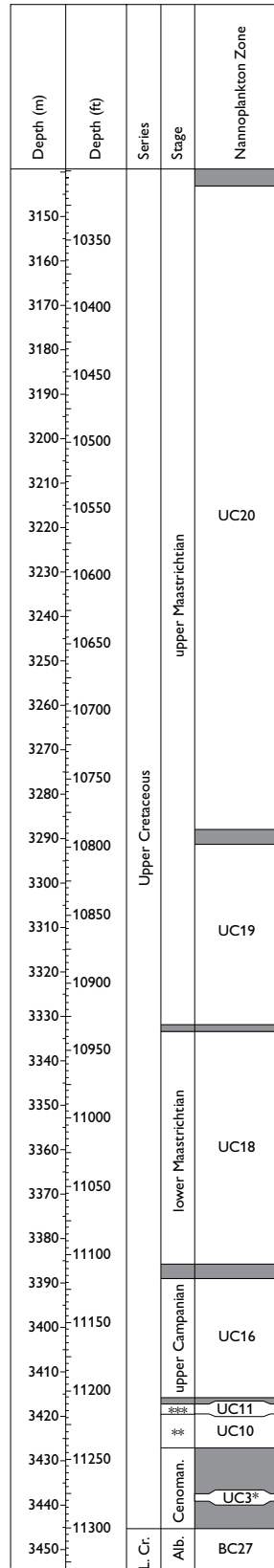The most logical and coherent lithostratigraphic scheme for the Upper Cretaceous in the North Sea appears to be that followed by Surlyk *et al.* (2003). This is essentially the scheme of Deegan & Scull (1977) with the modifications of Isakson & Tonstad (1989), but retaining the original distinction between the dominantly siliciclastic Shetland Group in the northern North Sea and the carbonate-dominated Chalk Group in the southern and central North Sea (Fig. 4). Few biostratigraphical studies have been undertaken on the Upper Cretaceous succession in Mona-1; the nannofossil zonation established for the well by Bailey *et al.* (1999) is used here (Fig. 5).

Materials and methods

The Mona-1 core is 331 m long and includes the uppermost part of the Lower Cretaceous Cromer Knoll Group and 303 m of the Upper Cretaceous Chalk Group. Core recovery was generally very high, except for a *c.* 12 m section in the upper part of the core. The core condition is excellent in the lower half of the Upper Cretaceous, whereas the porous upper part is in moderately good condition but very fragile and friable. The studied succession extends from the uppermost Albian to less than 10 m below the Cretaceous–Tertiary boundary at the top of the core.

A detailed core description was made at a scale of 1:5 or 1:15 in order to record the subtle sedimentary variations. A number of polished slabs were made, treated with light oil, and scanned at a resolution of 1200 dpi. This provides the equivalent of a 10-fold magnification at optimal resolution and allows for subsequent digital image processing such as contrast enhancement. All presented sedimentological logs are drawn in a naturalistic style, as close to the actual appearance of the core as possible. Trace fossils are identified to generic level. Twenty-five thin sections were produced for petrographic analyses. Porosity and permeability data were obtained from the conventional core analyses performed in 1983.

The original plug and drilling data are reported in imperial units, which were also used during core description to minimise the risk of error. Depths were subsequently converted to metric units and both types of units are reported throughout the manuscript.

Facies analysis

Definitions and terminology

Descriptions and interpretations of facies are summarised in Table 1. Some of the facies described below would probably be recognised as representing a continuum if studied in outcrop; such gradual change is very difficult to determine in core. A large number of facies was deliberately distinguished to prevent loss of information, as subtle differences have a potentially significant impact on the interpretation of the succes-

Table 1. Facies summary

Facies		Description	Interpretation
1	Bioturbated chalk	Completely bioturbated chalk with no preserved primary sedimentary structures.	Pelagite
2	Bioturbated marly chalk	Completely bioturbated marly chalk with no preserved primary sedimentary structures.	Pelagite
3	Laminated chalk	Chalk with vague and indistinct lamination seen as subtle colour differences.	Pelagites alternating with low-density turbidites and fall-out deposits from clouds of resuspended material
4	Laminated marl	Carbonate-rich siliciclastic mudstone with irregular, wispy and laterally discontinuous lamination.	Pelagite/hemipelagite
5	Graded silty chalk	Sharply based chalk with a relatively high concentration of silt-grade particles. Burrowed and rarely laminated.	Turbidite
6	Graded silty chalk with packstone lamination	Sharply based graded chalk with a relatively high concentration of silt-grade particles and fine sand to silt laminae.	Turbidite
7	Graded packstone and wackestone	Sharply based fine-sand packstone, which grades upwards into a fine sandy chalk wackestone.	Turbidite
8	Non-graded packstone and wackestone	Fine-sand packstone or fine sandy wackestone with a high density of burrows.	Turbidite
9	Structureless chalk	Structureless chalk, which may or may not be burrowed to a limited extent.	Mudflow deposit
10	Structureless matrix-supported chalk conglomerate	Structureless chalk or wackestone with randomly distributed and oriented matrix-supported fine sand to boulder-sized clasts, which may show coarse-tail grading.	Debrite
11	Clast-supported chalk conglomerate	Pebbly grainstone to pebble conglomerates composed of chalk clasts and subordinate shell debris.	High-density turbidite, derived from debris flow
12	Shear-deformed bioturbated chalk	Deformed chalk in which the bioturbated fabric is still recognisable.	Limited plastic deformation of bioturbated chalk
13	Shear-deformed matrix-supported chalk conglomerate	Matrix-supported chalk conglomerate with deformation structures.	Deformed debrite
14	Shear-banded chalk	Matrix-supported chalk conglomerate with irregular colour banding.	Intensely shear-deformed chalk

sion (Table 1). Texture is classified according to the modification of Dunham (1962) by Embry & Klovan (1971), with the further modification that mud is defined according to the Wentworth scale so that grains are particles larger than 63 μm. The terms 'silty' and 'sandy' are used solely to describe grain sizes and do not imply siliciclastic content. The terms 'plastic' and 'visco-plastic' are used according to mechanical definitions (Middleton & Wilcock 1994), i.e. 'plastic' is not synonymous with 'ductile' or 'soft'. The term 'bioturbated' is distinguished from the term 'burrowed' in this study. 'Bioturbated' is used here for extensively burrowed and biomottled deposits with no preserved primary sedimentary structures, such as lamination.

'Burrowed' is used for deposits that have been burrowed, but not to the extent that primary sedimentary structures have been totally obliterated. Fourteen facies are recognised, but Facies 12–14 are not facies in a classical sense, as they are defined by structures caused by penecontemporaneous deformation. However, they are defined as facies here because the occurrence of soft sediment deformation is critical for the interpretation of the succession. Also, it is in some cases impossible to determine whether the penecontemporaneous deformation was purely post-depositional or part of the depositional process. The primary lithological discriminator is the distinction between chalk, marly chalk, and marl (Plate 1). Chalk is defined as a rock or sediment that is compositionally dominated by calcareous nannofossils (Scholle 1977). In the studied succession, the chalk is a carbonate mudstone, and rarely a wackestone, and the main constituents of the carbonate mud are calcareous nannofossils with subordinate calcispheres and small foraminifers. Sand-sized bioclasts are mainly foraminifers, inoceramid shell fragments, and small fragments of bivalves, echinoderms, and other invertebrate fossils. The term marly chalk is used for chalk with a sufficiently high clay content to be recognised by its colour with the naked eye; the term marl is used for carbonate-bearing siliciclastic mudstones.

Facies 1: Bioturbated chalk

Description. This facies is characterised by its lithological composition and a completely bioturbated fabric with no preserved primary sedimentary structures (Figs 6, 7). The most common recognisable burrows are large and small *Chondrites* and *Planolites* and, less common, *Teichichnus* and *Taenidium*. *Zoophycos* is largely restricted to the 3288–3284 m (10 788 ft – 10 774 ft) interval, and possible *Thalassinoides* burrows mainly occur in the upper half of the core. The facies most commonly has a mudstone texture and may contain few scattered sand-sized bioclasts. In rare cases, local wackestone texture occurs due to the concentration of bioclasts. Lower boundaries are commonly gradational to the underlying facies, whereas upper boundaries are most commonly sharp. The facies constitutes a little more than one third of the entire succession and individual facies units are up to 6.3 m thick. It occurs throughout the succession, but it is most important in

the Maastrichtian part. It is commonly interbedded with Facies 5–8 and less commonly with Facies 3 and 4.

Intrapelagic erosion surfaces are important features intimately associated with Facies 1. They are sharp surfaces occurring within bioturbated chalk intervals, typically expressed by a subtle but abrupt change in colour. The surfaces appear to be smooth but may show a slightly wavy topography. They truncate burrows of the underlying unit, but may be penetrated by burrows descending from the overlying chalk. There are no significant changes in composition or texture associated with the surfaces. A total of 27 intrapelagic erosion surfaces are recognised, restricted to the lower half of the studied succession and strongly concentrated in the 3360–3325 m (11 030 ft – 10 910 ft) interval. They are most common within pelagic units that include relatively few, thin and fine-grained interbeds belonging to Facies 5–8.

Interpretation. The complete lack of primary structures and the thoroughly bioturbated fabric indicate fully oxygenated benthic conditions and relatively slow accumulation. These conditions allowed the infauna to continuously burrow the sea-floor sediments and destroy all primary structures. The range of trace fossil tiers and the rarity of benthic fossils indicate a relatively rich infauna and a restricted shelly epifauna, which suggests a high nutrient flux to the sea floor (Dayton & Oliver 1977; Bambach 1993; McKinney & Hageman 2006). The original depositional process cannot be determined due to the destruction of primary structures, but the slow accumulation indicates deposition mainly by pelagic fall-out although a contribution from thin event beds is likely (see Facies 3).

The lack of mineralisation or lags in association with intrapelagic erosion surfaces indicates that they do not represent significant time intervals, but rather appear to represent short perturbations of the pelagic deposition by sediment gravity flows or bottom currents; the latter are increasingly being recognised as an important influence on relatively deep-water chalk deposition (Lykke-Andersen & Surlyk 2004; Esmerode *et al.* 2007, 2008; Surlyk & Lykke-Andersen 2007; Surlyk *et al.* 2008; Esmerode & Surlyk 2009). The lack of lags and characteristic event deposits suggests that the eroded material was transported away from the site, rather than being resuspended locally and producing a post-event, fall-out deposit. The amount of erosion is difficult to assess in a core, but the fact that the surfaces are preserved implies that the soft uppermost part of the

Fig. 6. Typical appearance of bioturbated chalk (Facies 1; 3360.02–3359.87 m, see Plate 1). Note the mottled appearance due to the numerous superimposed vaguely defined colour variations.

1 cm

sediment column, where the most efficient burrowing organisms would have prevailed, was removed by erosion. Deep burrowers adapted to firm, somewhat compacted sediment (e.g. *Chondrites*) were not excluded, however, indicating that erosion probably proceeded to a depth of a few tens of centimetres.
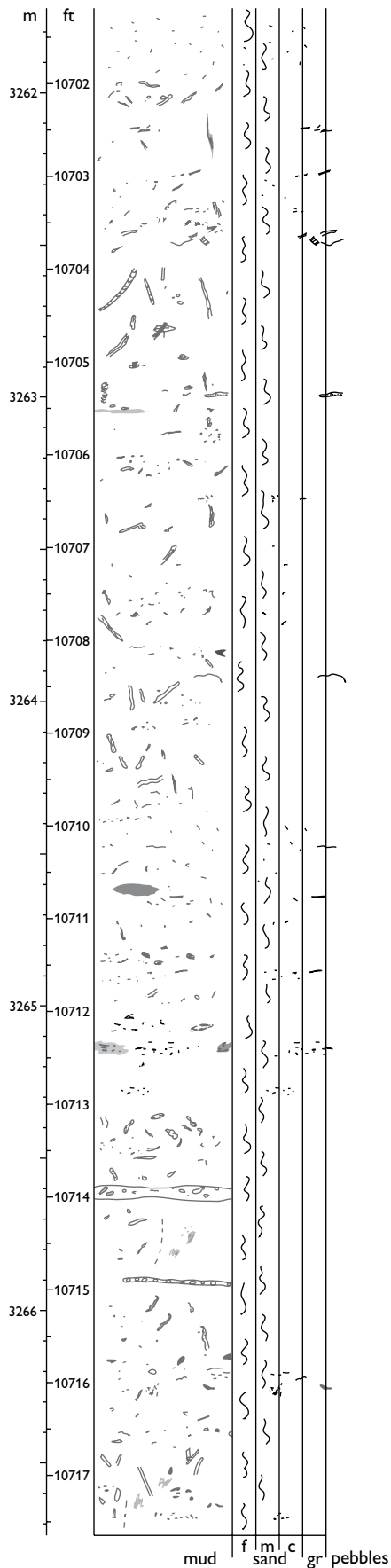
Facies 2: Bioturbated marly chalk

Description. This facies comprises completely bio-turbated chalk with a siliciclastic mud content large enough to be detected by its colour with the naked eye (Figs 8, 9). The ichnofabric is dominated by small *Chondrites*, *Zoophycos*, *Planolites*, with less common large *Chondrites* and *Taenidium*. The facies only occurs in a 3.15 m thick interval in the Cenomanian part of the core, where it transitionally overlies laminated marl (Facies 4).

Interpretation. The thorough bioturbation indicates relatively slow pelagic carbonate and hemipelagic clay accumulation under well-oxygenated benthic conditions. The prevalence of *Zoophycos* may indicate relatively stable conditions and slow continuous deposition in deep water (Ekdale & Bromley 1984).

Fig. 7. Typical bioturbated succession showing random distribution of bioclasts and recognisable trace fossils, mostly *Planolites*, *Chondrites*, some *Teichichnus*, and one possible *Thalassinoides*.
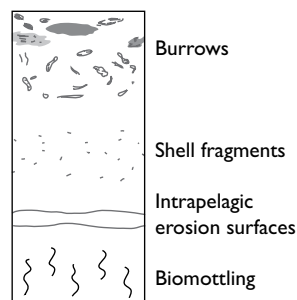

14

Fig. 8. Bioturbated marly chalk (Facies 2; 3441.50–3441.24 m, see Plate 1) with a mottled appearance and prominent *Zoophycos* (arrows).
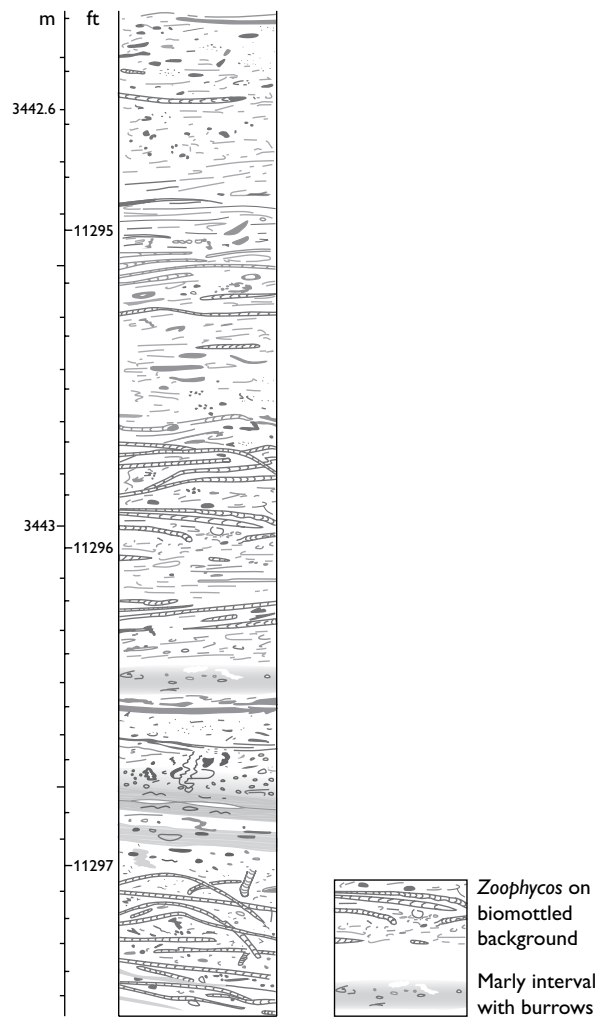
Fig. 9. Log example of bioturbated marly chalk (Facies 2). Note the intensely bioturbated fabric dominated by small *Chondrites*, *Zoophycos* and *Planolites*.

Facies 3: Laminated chalk

Description. This facies is characterised by vague and indistinct lamination expressed as subtle colour differences (Figs 10, 11). The laminae are 1–10 mm thick, planar, commonly laterally discontinuous, and low-angle cross-cutting relations between laminae have been observed. The laminae are not visible under the microscope, as there are no obvious differences in grain size, composition or texture. The cause for lamination must thus be variations on the nannofossil scale. In rare cases, the laminae appear to be inversely graded, and small-scale dish structures also occur.

It is common to find diagenetic lamination induced by slight pressure dissolution in association with true lamination. True lamination is distinguished from diagenetic lamination by being cut by burrows and lacking signs of pressure solution and concentrations of dissolution residues. Some units are devoid of burrows, but burrows commonly occur in small numbers. *Chondrites* and small *Planolites* are by far the most common, but *Teichichnus* has also been observed. The facies makes up a total of 5.5 m distributed over 37 occurrences throughout the core and individual units are 2–150 cm thick. Eight units are thicker than 30 cm, 12 are 5–30 cm thick, and 17 are thinner than 5 cm. Most of the units thicker than 30 cm are overlain by redeposited facies, and a little more than half of the 5–30 cm thick units are overlain by redeposited facies, whereas most of the thin units are overlain by bioturbated facies.

Interpretation. The lamination was probably formed by deposition from low-density turbidity currents alternating with pelagic fall-out and settling from clouds of suspended material (Damholt & Surlyk 2004). The suspended material may have been resuspended by currents or waves or lofted from sediment gravity flows. All these processes produced thin laminae or surfaces which would rapidly have been destroyed by bioturbation under oxygenated benthic conditions. The preservation of lamination and the lack of bioturbation were thus interpreted by Damholt & Surlyk (2004) to have been the result of dysoxia at the sea floor during deposition. Other authors have interpreted such laminated chalk beds to have formed by rapid deposition, the high sedimentation rate precluding thorough bioturbation (Scholle *et al.* 1998). The depositional process and the cause for the lamination according to this latter model are unclear, however, and the interpretation of Damholt & Surlyk (2004) is thus preferred here.

The fall velocity of coccoliths and microfossils, such as calcispheres and foraminifers, differ by two orders of magnitude (McCave 2008), and deposition from dilute suspension clouds or turbidity flows may therefore be expected to have produced clear distribution grading, a feature not observed in this laminated chalk facies of the Mona-1 core (see also Damholt & Surlyk 2004). There may be several explanations for the lack of well-defined distribution grading. Lofted flows and nepheloid layers would probably consist of only very fine grains, thus having a too limited grain-size range to produce visible

Fig. 10. Laminated chalk (Facies 3; 3386.01–3385.93 m, see Plate 1). The image shows both primary (large arrows) and diagenetically enhanced lamination (small arrows); note that primary lamination passes laterally into diagenetic lamination in some cases. Burrows occur throughout.
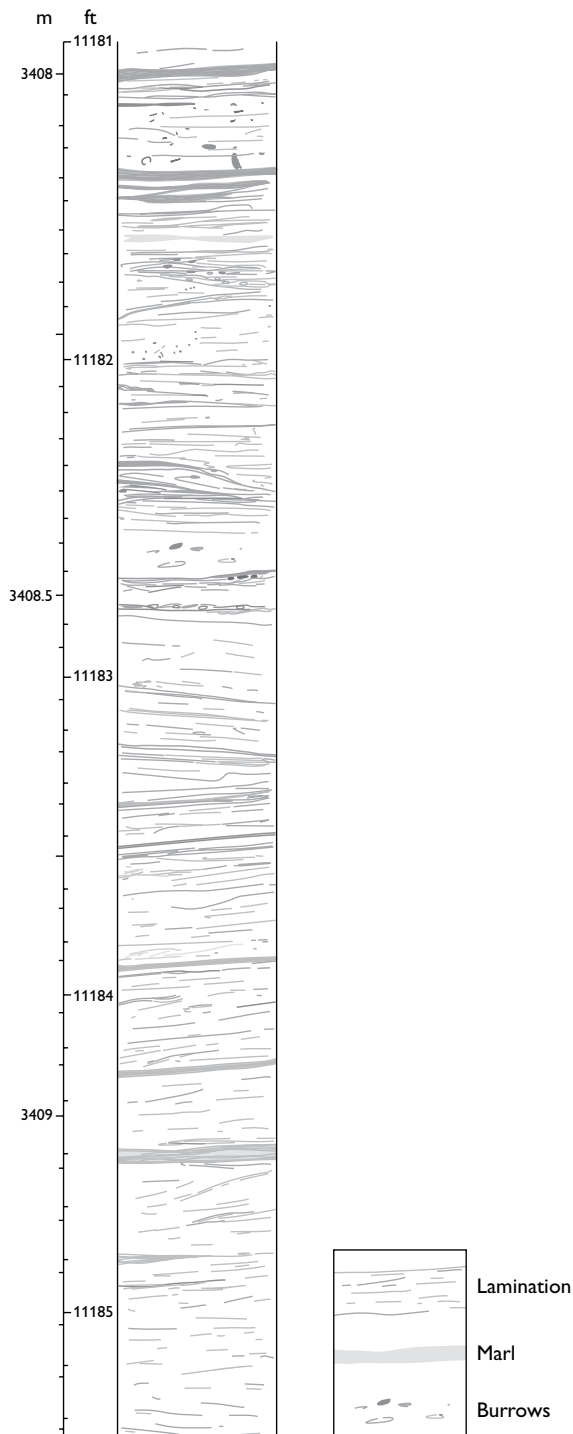
Fig. 11. Log example of laminated chalk (Facies 3, see Plate 1) alternating with thin beds of laminated marl (Facies 4). Note the irregularity of the lamination. The marl beds are invariably associated with pressure dissolution.

distribution grading. Indeed, the finest parts of other chalk turbidites studied here, consisting largely of coccoliths and calcispheres, typically do not show marked distribution grading. It must be borne in mind that although chalk ooze is commonly referred to as 'completely non-cohesive' due to the lack of clay minerals, almost nothing is known about the physical properties of the ooze in its original form. Van der Waals forces, organic material such as extracellular polymeric substances, grain morphology and non-preserved spiculate material are all potentially highly influential factors in this respect. Thus, particle aggregation may have been a significant factor in such fine-grained suspensions, and this in turn may have significantly influenced the resultant grain-size distribution after the removal of labile material.

The close association between the thickness of laminated units and the type of overlying deposits suggests a causal link. If deposition took place during dysoxia and was followed by similar deposition under oxygenated conditions, burrowing organisms would penetrate downwards into the laminated sediment, thereby destroying the lamination and reducing the thickness of the laminated unit. However, the full thickness of the laminated unit would be preserved if the unit was capped by redeposited chalk. This may explain why thick laminated units are commonly overlain by redeposited facies, whereas thin laminated units are typically overlain by bioturbated facies.

Facies 4: Laminated marl

Description. This facies comprises carbonate-rich siliciclastic mudstone with irregular, wispy, and laterally discontinuous lamination (Fig. 11). It makes up a total of 3.60 m of the studied succession and occurs at four different levels and in three somewhat different fashions. The lowermost part of the studied succession is a laminated marlstone with abundant *Chondrites* and common *Planolites*. It passes upward into bioturbated marly chalk at the Albian–Cenomanian transition. The facies also occurs at 3423.7–3422.7 m (11 232 ft 8 in. – 11 229 ft 4 in.) where it transitionally overlies a 46 cm thick turbidite (Facies 6). In this unit, the lamination is less well preserved due to the abundance of shallow tier *Planolites* and *Taenidium*. In two other cases in the 3411.6–3408.0 m (11 193 ft – 11 181 ft) interval,

laminated marl occurs as numerous diagenetically enhanced layers interbedded with laminated chalk. The marl layers are invariably associated with dissolution features, and they are generally *c*. 1 cm thick.

Interpretation. The units belonging to this facies may have polygenetic origins. The lowermost example is interpreted to represent hemipelagic and some pelagic deposition during oxygen-deficient benthic conditions. The occurrence at 3423.7–3422.7 m (11 232 ft 8 in. – 11 229 ft 4 in.) appears to represent deposition from dilute mud suspension following deposition of the underlying turbidite. The thin dissolution marl laminae associated with laminated chalk may represent primary marl layers, or they may simply be pressure-solution products of originally slightly argillaceous chalk.

Facies 5: Graded silty chalk

Description. This facies is conspicuous due to its pale colour, in contrast to the dominantly light grey colour of the surrounding chalk (Fig. 12). Beds are 1–22 cm thick and invariably occur within bioturbated intervals; they are typically heavily burrowed and their primary structures are only partially preserved. The facies has a relatively high concentration of silt-grade and more rarely fine sand-grade particles, mainly calcispheres (Fig. 13A). Where preserved, beds show a subtle overall grading with 0.5 mm thick silt laminae. The laminae have high concentrations of calcispheres and rarer small foraminifers, both of which are typically filled with pyrite or calcite, giving the laminae a black coloration (Figs 12, 13A). Lower boundaries are sharp or burrowed, and upper boundaries are invariably burrowed. There are 35 beds of Facies 5 in the core, principally in the 3378.6–3324.1 m (11 084 ft 9 in. –10 905 ft 10 in.) interval.

1 cm
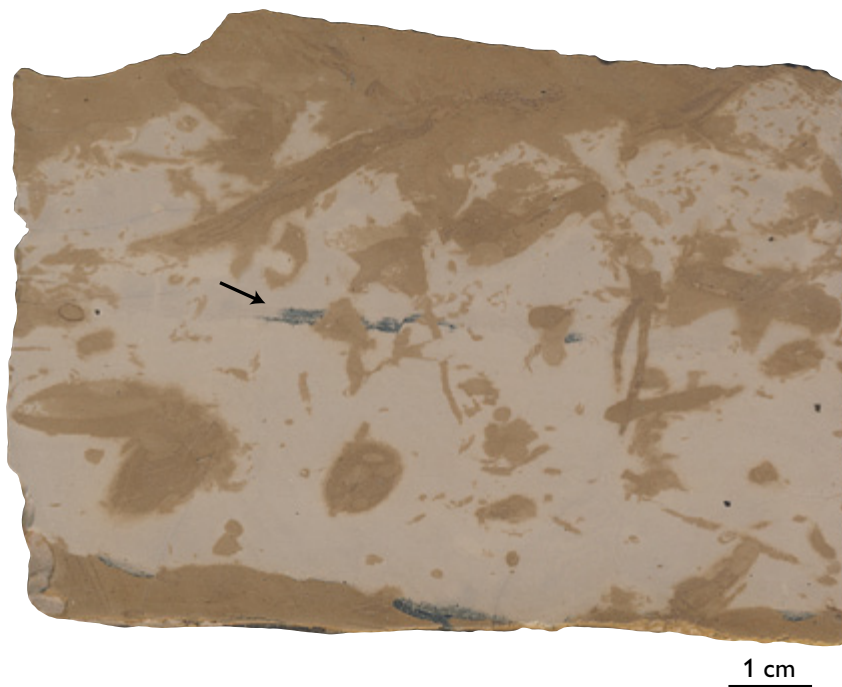
Fig. 12. Graded silty chalk (Facies 5; 3369.44–3369.36 m, see Plate 1), which has a conspicuous pale colour and is burrowed. The black parts represent remnants of silty lamination heavily cemented by pyrite (arrow).

Fig. 13. Photomicrographs (plane polarised transmitted light) of thin sections. **A**: Silty laminae in graded silty chalk (Facies 5; 3369.40 m, see Plate 1). Note absence of intraparticle porosity due to pyrite and calcite cement. **B**: Silt to fine sand lamina in graded packstone and wackestone (Facies 7; 3284.36 m, see Plate 1) showing well-developed intraparticle cement.
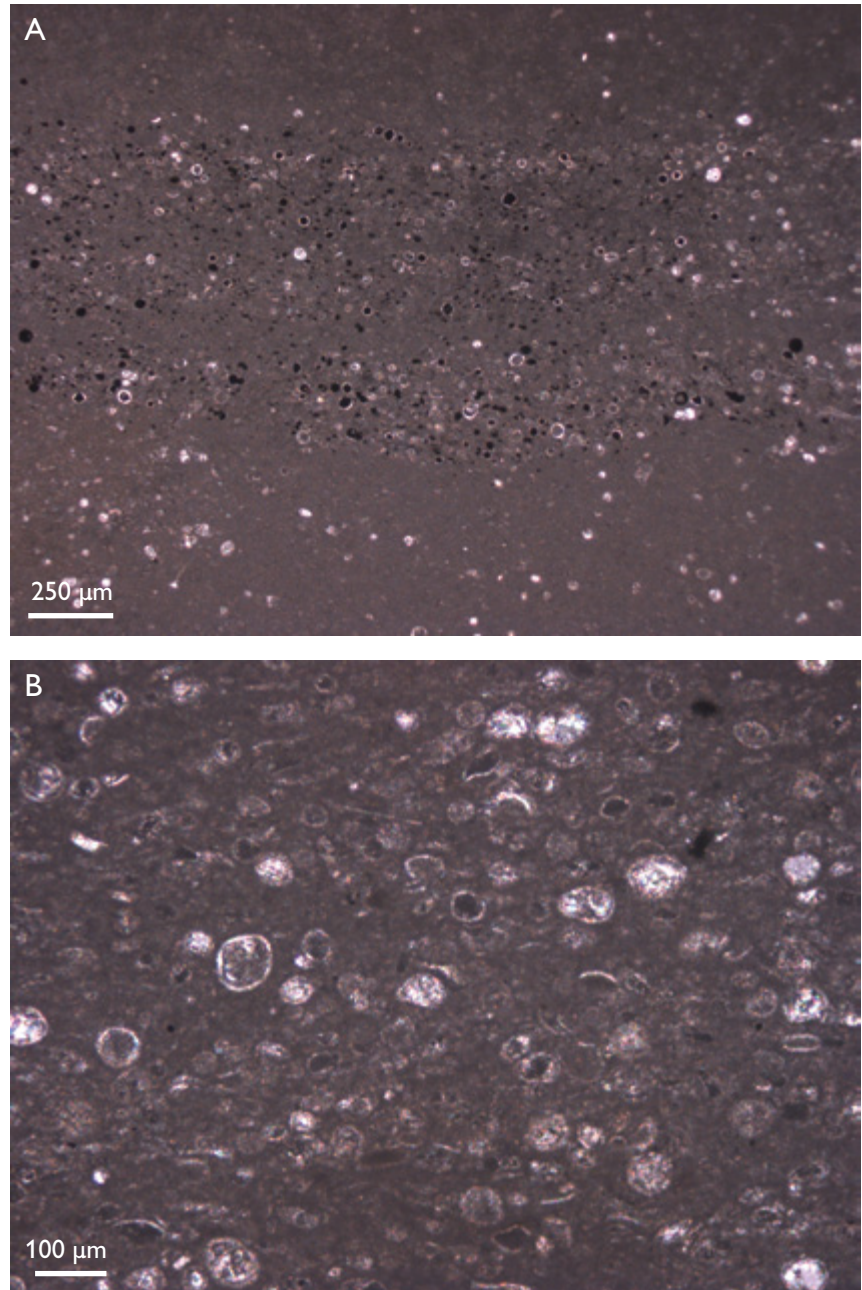
Interpretation. The sharp base, overall grading and graded silty laminae all indicate that the facies represents silty mud-grade carbonate turbidites, which due to their limited thickness were heavily burrowed subsequent to deposition. In terms of standard turbidite models, the facies is analogous to the lower part of the E division of Bouma (1962), the upper part of E_1 of Piper (1978), or the T_2–T_4 divisions of Stow & Shanmugam (1980).

1 cm

Facies 6: Graded silty chalk with packstone lamination

Description. Facies 6 is composed of chalk, and silt to fine sand-grade pelagic bioclasts and fragments of benthic invertebrate fossils. The 10–45 cm thick beds all have sharp and commonly loaded bases (Figs 14, 15), which truncate burrows of underlying facies. The base is typically overlain by a graded and in some cases laminated sandy interval a few centimetres thick (Fig. 16). The basal interval grades upwards into a graded silty chalk interval with discrete fine sand to silt laminae that show upwards decreasing, lateral continuity, thickness and regularity. The laminae are reduced to thin, indistinct silty lenses towards the top of the beds. The graded silty chalk interval makes up the greater part of the beds. One ripple form set and several examples of small-scale dish structures have been recorded. The top of the beds may comprise a relatively thin structureless chalk interval grading into bioturbated chalk, or the graded chalk may be overlain by a thick laminated chalk or marl that is burrowed at the top (Facies 3 and 4). The beds are not burrowed, except at the top when overlain by bioturbated chalk.

There are 13 beds referred to Facies 6, which make up a total of 3.18 m. All beds occur in the 3411.6– 3398.1 m (11 192 ft 9 in. – 11 148 ft 9 in.) interval, except for one at 3424.2 m (11 234 ft 2 in.). Thus, the facies occurs in association with Facies 7 and Facies 1, and three of the beds are overlain by the laminated Facies 3 and Facies 4.

Interpretation. The sharp erosional base, overall normal grading and succession of structures indicate that the facies represents fine sand to mud turbidites. They essentially correspond to the C–E divisions of Bouma (1962), E_1–E_3 of Piper (1978), and T_0–T_8 of Stow & Shanmugam (1980) although Facies 6 is starved of sand-sized particles compared to siliciclastic turbidites, which formed the basis for the standard facies models mentioned above. The siliciclastic examples are distal

Fig. 14. Graded silty chalk with packstone lamination (Facies 6; 3424.21–3423.84 m, see Plate 1). The lower part (bed base is indicated) contains several barely visible contorted sand-grade laminae, whereas lamination is more clearly visible in the upper part of the sample due to colour variations caused by porosity differences.
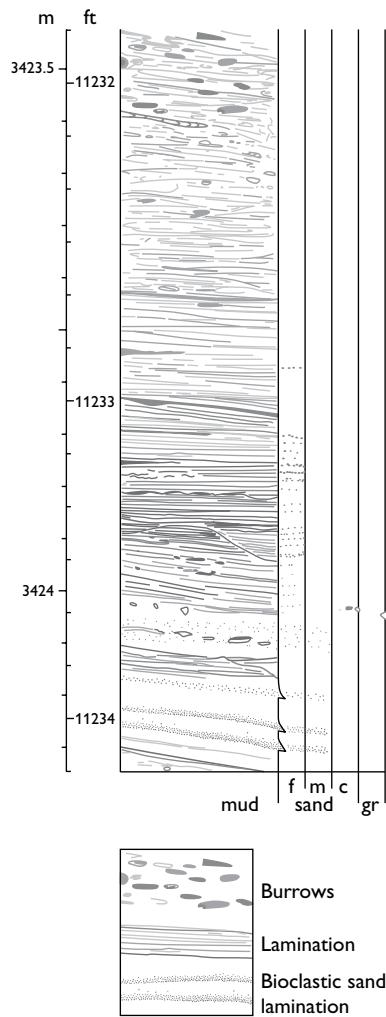
Fig. 15. Log example of a graded silty chalk bed with packstone lamination (Facies 6, see Plate 1). Bed base at 3424.13 m.

shelf- or delta-derived, outer-fan and channel-levee deposits, whereas Facies 6 was derived from pelagic chalk with a low content of sand-sized carbonate particles.

Fig. 16. Detail (**A**) and photomicrograph (**B**) of thin section of a lamina in Facies 6 (3407.13 m, see Plate 1). Note the normal grading in **B**. The dashed outline in **A** indicates the location of the thin section in **B**.
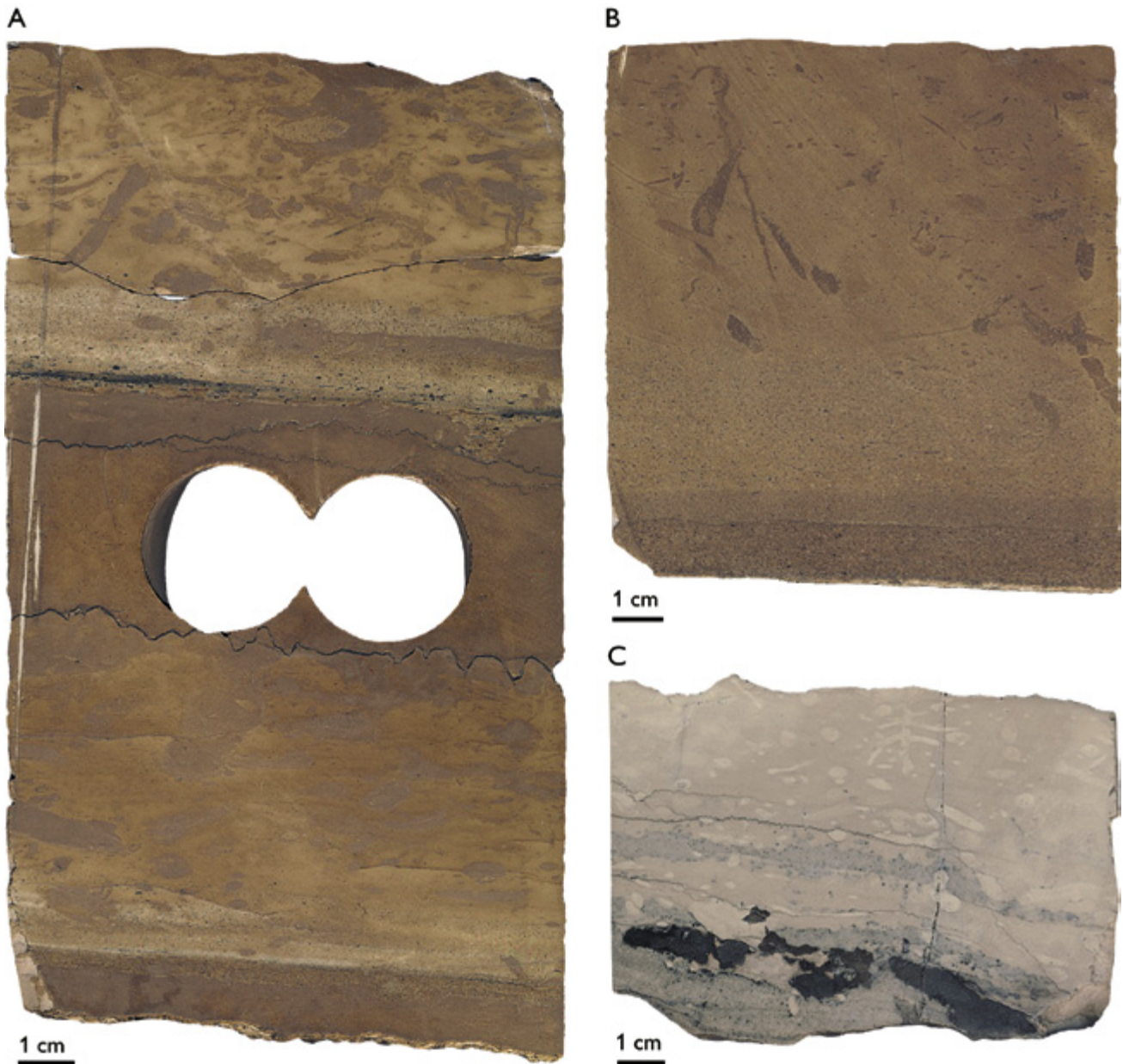
Fig. 17. Graded packstone and wackestone (Facies 7). **A**: Two thin sandy beds of Facies 7 units (3376.04–3375.86 m, see Plate 1) characterised by sharp bases, normal grading and top–down burrowing. **B**: A Facies 7 sample (3401.97–3401.87 m, see Plate 1) with a relatively thick, laminated sand-grade base. **C**: Facies 7 example (3284.40–3284.32 m, see Plate 1) with heavy pyrite staining. Sand-sized bioclasts are commonly filled by pyrite cement in all three examples, but the cementation is especially conspicuous in **C**.

Facies 7: Graded packstone and wackestone

Description. This facies may be regarded as equivalent to the lower, graded sandy interval of Facies 6 being characterised by sharply based packstone which grades upwards into chalk wackestone (Fig. 17). It consists of silt to fine-grained pelagic carbonate sand and pelagic mud, together with benthic bioclastic debris which is mostly up to fine sand grade although slightly coarser

bioclasts do occur. Faint parallel lamination is relatively common and ripple cross-lamination occurs in one unit. Burrows are common in the top of the beds but rare in the basal part. The lower boundaries are invariably sharp and truncate underlying structures, whereas upper boundaries are gradational unless truncated by another bed belonging to Facies 5–8. Facies 7 is commonly partially stained black by pyrite and thin sections invariably show well-developed intraclastic cementation (Fig. 13B). Facies 7 almost always overlies, and is overlain by, bioturbated chalk of Facies 1. There are 40 Facies 7 beds making up a total of 2.62 m in the core, with individual beds being 1–18 cm thick.

Interpretation. Facies 7 beds are interpreted as turbidites on the basis of the sharp, erosional lower boundary, normal grading, horizontal lamination, rare ripple cross-lamination, and top-down burrowing. The facies belongs to the C division of Bouma (1962), the basal part of E_1 of Piper (1978), or the T_0 division of Stow & Shanmugam (1980). In many cases, the facies resembles the basal part of Facies 6, the main difference being that Facies 7 is slightly thicker and sandier than the basal part of Facies 6, and that it lacks the relatively thick muddy interval with sandy laminae that dominates Facies 6.

Facies 8: Non-graded packstone and wackestone

Description. This facies is represented by thin beds of fine sand packstone and more rarely wackestone. The composition is identical to that of Facies 7. The facies is normally a few centimetres thick, shows a high density of burrows, and lower and upper boundaries are transitional to fully bioturbated chalk (Facies 1), except in two cases where it is associated with redeposited facies and where Facies 8 shows no burrows and is sharply bounded by thin zones of intense shear deformation. There are 26 occurrences of the facies making a total of 80 cm, almost all of which are found in the pelagite/turbidite dominated interval in the lower half of the core (3411.6–3324.1 m, 11 192 ft 9 in. – 10 905 ft 10 in.).

Interpretation. Facies 8 is identical to Facies 7 in terms of composition and grain size, but lacks grading, sharp boundaries and sedimentary structures. It is interpreted

to represent thin, fine sand-grade turbidites, equivalent to Facies 7, which were homogenised by bioturbation, or in rare cases by shear deformation. Burrowing generally affected only the top part of Facies 7, whereas the generally thin Facies 8 units suffered complete biogenic reworking. The bioturbation destroyed grading and other structures, blurring the sharp boundaries and, in some cases, resulting in mixing of the turbidite sand and chalk ooze and the creation of a wackestone texture. More rarely, the homogenisation was caused by shear deformation rather than bioturbation. The facies belongs to the C division of Bouma (1962), the basal part of E_1 of Piper (1978), or the T_0 division of Stow & Shanmugam (1980).

Facies 9: Structureless chalk

Description. This facies is a structureless chalk, which may be burrowed to a limited extent (Fig. 18). It may contain fine sand-grade bioclasts and rare randomly distributed and oriented benthic fossil fragments. In some cases, the facies shows subtle signs of deformation represented by vague, folded colour-bands. It does not show the mottled appearance that characterises the bioturbated chalk facies. Burrows are typically few and concentrated at the top of individual beds. The most common burrows are small *Chondrites*, whereas *Planolites*, *Taenidium*, and *Teichichnus* occur in subordinate numbers. *Trichichnus*, which is very rare in the other facies, is relatively common. Some Facies 9 intervals show internal burrowed surfaces from which burrows penetrate down into the underlying bed, whereas the overlying beds are devoid of burrows, indicating that the interval is amalgamated and composed of several individual units. Lower boundaries are typically transitional over a short vertical distance and therefore appear abrupt. There are 28 units of the facies, which mainly occur in intervals characterised by extensive redeposition. Individual units are 2–815 cm thick, and make up a total of 23 m. Most units are less than 30 cm thick and are interbedded with laminated chalk (Facies 3). Units thicker than 1 m overlie Facies 10 or Facies 12–14. The lowermost unit is 8.15 m thick, overlies deformed bioturbated Facies 12 and shows scattered burrows, although very few, throughout the unit.
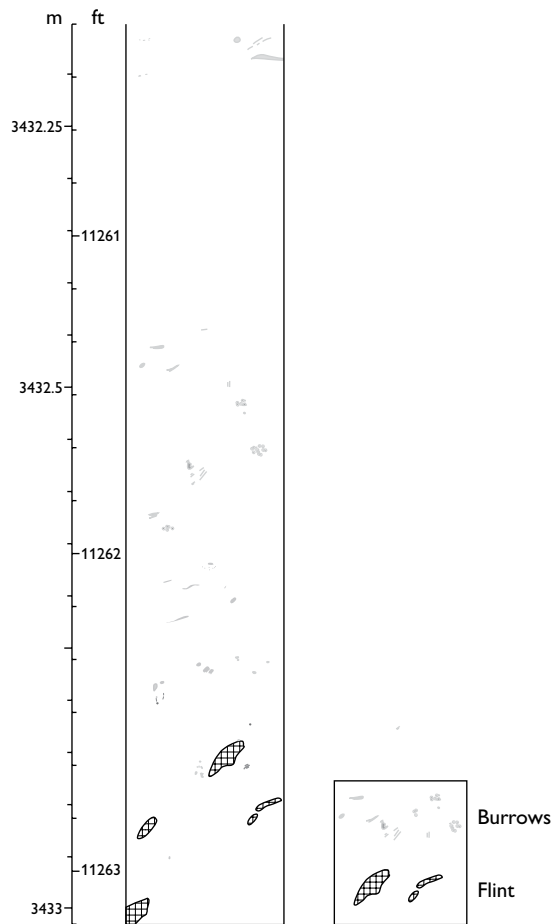
Fig. 18. Log example of structureless chalk (Facies 9, see Plate 1). Although not bioturbated, a few isolated burrows are evident.

Interpretation. The structureless appearance is considered a primary sedimentological feature, although it cannot be ruled out in all cases that the lack of sedimentary structures or burrows is simply due to a lack of colour contrast within the material. The facies is most commonly overlain by thinner laminated chalk units of Facies 3, however, which may suggest a genetic relationship. Also conspicuous is the common association with deformed or redeposited units. In addition, most units are burrowed at their top only, with burrows increasing in density toward the top, indicating that burrowing took place after deposition. The structureless appearance indicates rapid deposition excluding any sorting or structuring of the chalk ooze. The facies may thus be interpreted to have been deposited by mudflow, which is essentially a clast-free debris flow. The lack of

clasts may be attributed to a lack of coherence in the source material, or that the flow was too dilute to possess sufficient shear strength to support clasts. The very thick unit in the lower part of the succession (Plate 1, 3434.5–3426.4 m) is burrowed, although to a limited extent, throughout its 8.15 m of thickness, and is interpreted to have been deposited at a rate roughly equal to the rate of burrowing, which points towards deposition from a high-concentration suspension cloud or to the amalgamation of several flows. All observations taken together indicate that Facies 9 beds were deposited by high-concentration gravity-driven suspension flows, which formed dilute visco-plastic flows during the final stages of deposition.

Facies 10: Structureless matrix-supported chalk conglomerate

Description. This facies consists of a structureless chalk mudstone or more rarely wackestone matrix with dispersed fine sand- to boulder-sized clasts, which are typically randomly distributed and oriented but may show coarse-tail grading (Figs 19, 20). Burrows are absent or restricted to the top of individual units. The facies makes up a total of 30.5 m distributed over 16 units, varying in thickness from 15 cm to 19 m. Thin units generally occur within intervals dominated by Facies 1–8.

The clasts may be divided into chalk clasts, other lithic clasts, and bioclasts (Fig. 21). Chalk clasts are abundant, white to light grey, medium sand- to boulder-sized, although most are granule- to pebble-sized. They are mainly rounded to subangular. Some chalk clasts show smear-structures ranging from minute flame-like structures extending subhorisontally from the clast surface into the matrix, over bidirectional double tails, to completely streaked-out clasts, forming thin white and commonly folded bands. Incipient rip-up clasts, recognised as angular chalk clasts immediately above similarly shaped cavities in the underlying bed, have been observed at the base of redeposited units. Many chalk clasts in thick units are considerably richer in fossils than the surrounding pelagic chalk, with bryozoan and small shell fragments making up the bulk of the fossils. A few hardground clasts have been observed. Fossil-rich chalk clasts may show surfaces with punctate irregularities reminiscent of borings, but these surface
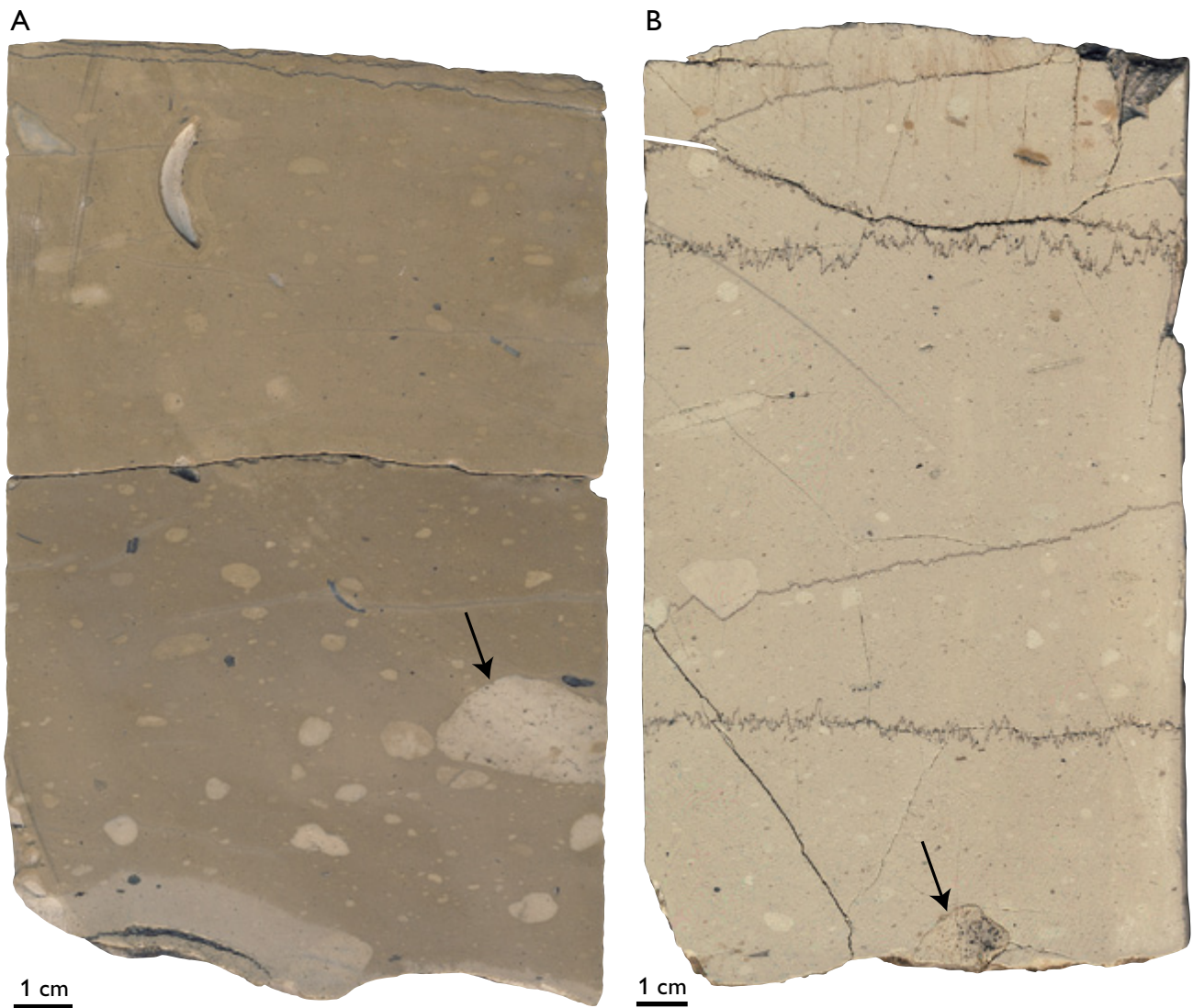
Fig. 19. Typical appearance of a structureless matrix-supported chalk conglomerate (Facies 10; **A**: 3363.01–3362.89 m. **B:** 3247.59–3247.42 m (see Plate 1). The sample in **A** was treated with light oil for colour-contrast enhancement. Note the prevalence of subangular white chalk clasts. Dark bioclasts (mostly inoceramid fragments) and a few large chalk wackestone clasts are also present (arrows). The crescent-shaped structure in the upper left part of **A** is a drill mark made from plug sampling.

structures are moulds of small fossil fragments which were chipped off the clast during redeposition or possibly dissolved. Other lithic clasts are rare and include green sand- and siltstone clasts, shale chips, and small round to elongate glauconitised chalk clasts. Bioclasts are dominated by bivalve shell debris, especially sand- to fine pebble-sized inoceramid fragments. Foraminifers make up an important but less conspicuous group, and bryozoan fragments occur in thicker units. Other observed but rare bioclasts are from brachiopods, echinoderms, sponges, belemnites, and corals.

A typical unit has a light grey, porous matrix, in contrast to the white and less porous medium sand- to coarse pebble-sized chalk clasts. The matrix itself is structureless, but the clasts are coarse-tail graded in some units. One notable exception is the lowermost occurrence of the facies, which is a *c.* 5 m thick reddish coarse-tail graded inoceramid chalk wackestone with boulders composed of bioturbated marly chalk (Facies
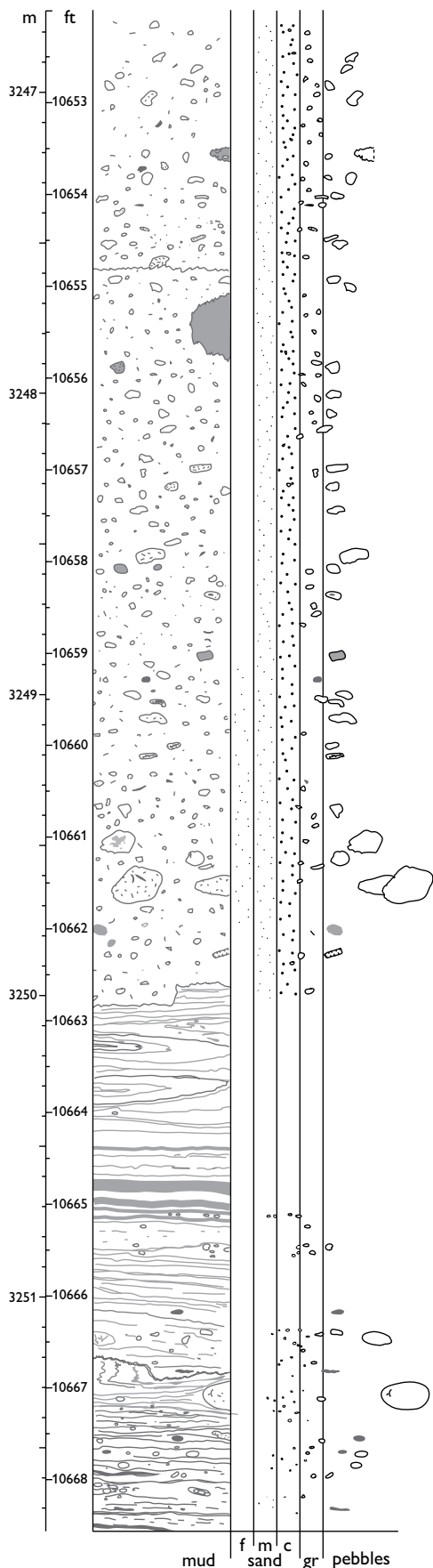
2), which most likely originated from the underlying lowermost Cenomanian (Fig. 22). The matrix is relatively fossil-rich and appears to be derived from a more shallow-water facies than the underlying and overlying chalk. The boulders are highly fractured and show numerous internal discordant surfaces. The fractures are not expressed by the boulder surface morphology, indicating that fracturing took place prior to emplacement. Three 20–25 cm thick units in the 3411.6–3378.6 m (11 192 ft 9 in. – 11 084 ft 9 in.) interval, which is dominated by Facies 1–8, constitute another variant of Facies 10. They consist of coarse-tail graded, completely glauconitised medium sand- to granule-sized, oval clasts in a structureless mudstone matrix. One of the units is directly overlain by Facies 8, and the two others are overlain by Facies 3.

Basal surfaces can only be examined in nine out of the sixteen units due to stylolites or poor core preservation; all but one of the nine units are sharply based. Two of the basal surfaces are clearly erosional and two others are marked by thin shear zones. Upper boundaries may be sharp or gradational, depending on the overlying facies. Units with burrowed tops may grade into bioturbated chalk (Facies 1) and units occurring within deformed intervals may grade into shear-deformed, matrix-supported chalk conglomerates (Facies 13), although the transition may also be quite abrupt. Upper boundaries are sharp when overlain by Facies 5–8 or laminated chalk (Facies 3).

Interpretation. The matrix-supported clasts indicate deposition by 'freezing' of a flow with some shear

Fig. 20. Shear-banded chalk (Facies 14, lower part) overlain (at *c.* 3250 m) by a structureless matrix-supported chalk conglomerate (Facies 10); the two facies are separated by a stylolite surface. The colour banding in the upper part of the Facies 14 unit shows tight to isoclinal folds.

Chalk clasts and shell fragments

Shear banding
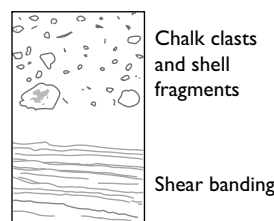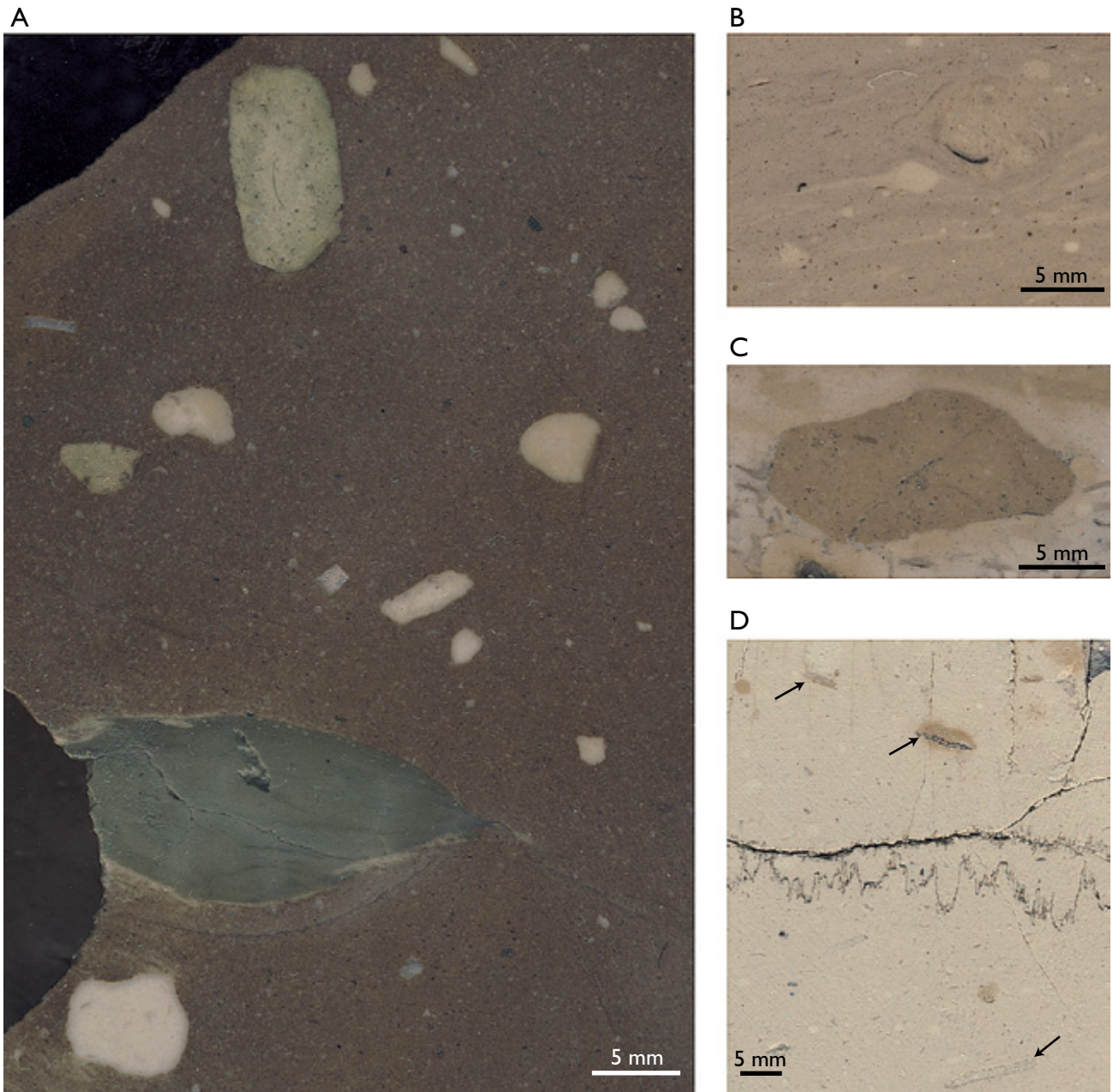
Fig. 21. Clasts associated with Facies 10, 11, 13 and 14. **A**: White subangular chalk clasts are the most common type of clast, but note also the large green marl clast in the lower part of the image and a greenish packstone clast in the uppermost part of the image. From 3422.65 m (see Plate 1) **B**: Common appearance of chalk clasts in Facies 14. Note the small size of the clasts and white streaks extending laterally from the clasts. The 3 mm long dark object is an inoceramid fragment. From 3325.25 m (see Plate 1). **C**: Exotic chalk clast rich in bioclasts (mostly small inoceramid fragments). From 3361.87 m (see Plate 1). **D**: Fragments of bryozoan colonies (arrows) within a structureless matrix-supported chalk conglomerate (Facies 10). From 3247.42 m (see Plate 1).

strength, and the structureless matrix indicates total homogenisation during flow but sudden deposition in the absence of a sorting mechanism. The material must thus have possessed both fluid-like properties during flow and plastic properties during deposition. This type of visco-plastic, or Bingham plastic, rheology is a well-

documented feature of debris flows (Johnson 1970), in which a relatively high-concentration sediment–water mixture, flowing under the influence of gravity, is able to support clasts much larger than the individual matrix components. Chalk debris flows must have been formed by failure of chalk, whereupon relatively unconsolidated material was completely mixed with water until reaching a fluid state, whereas more consolidated and perhaps somewhat cemented material disaggregated to form chalk intraclasts. Deeply buried, fully lithified chalk was thus rarely reworked into debris flows, and hardground clasts are rare exceptions.
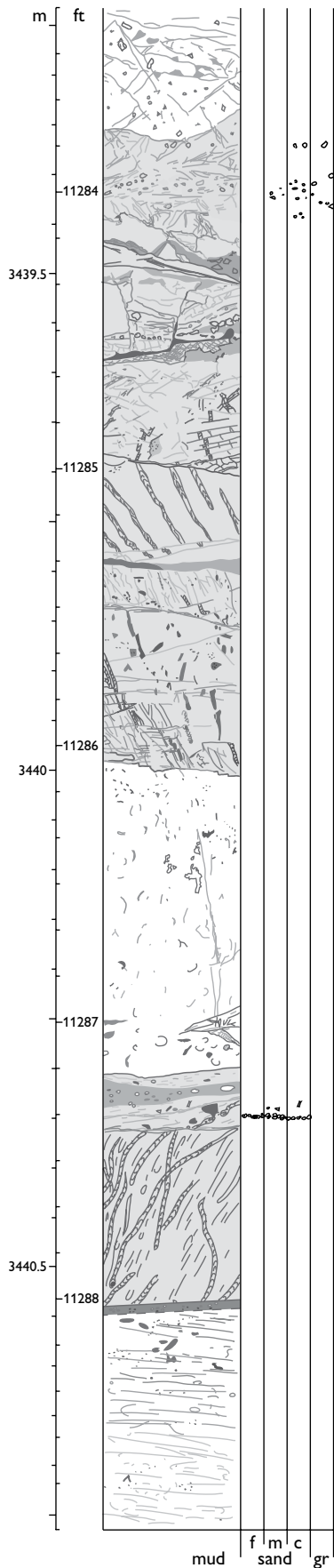
Fig. 22. Lower part of a structureless matrix-supported chalk conglomerate (Facies 10) with boulder-sized clasts (dark tone) similar to the underlying bioturbated marly chalk (see also Plate 1). The base of the unit just below 3440.5 m is marked by an argillaceous shear zone. The boulders were subjected to intense fracturing and welding prior to redeposition.

Boulder-sized clasts

Subvertical *Zoophycos*

Shell fragments

Burrows and faint lamination

Fractures
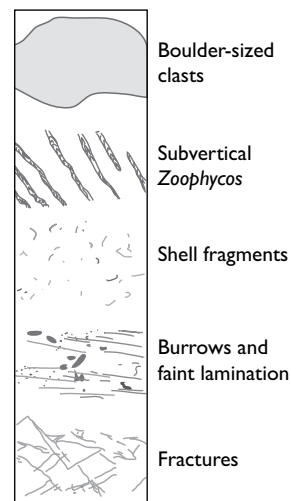
Facies 11: Clast-supported chalk conglomerate

Description. This facies is characterised by granule–pebble grade, clast-supported conglomerates but also includes pebbly grainstone beds. Chalk clasts dominate, with subordinate shell debris (Figs 23, 24). Units belonging to this facies have sharp and loaded bases, whereas the upper boundary may be sharp or gradational, depending on the grain size. There is a range of variation within the ten units referred to Facies 11. Four units are 2–8 cm thick and are composed of roughly equal amounts of chalk clasts and shell debris in the coarse pebble to coarse sand fraction. These units show normal or inverse-to-normal grading. Four other units are relatively fine-grained, with clast sizes ranging from granule chalk clasts to fine sand bioclasts with rare pebbles. The units are normally graded or inverse-to-normally graded, with the rare pebbles occurring randomly without reference to the overall grading. They typically grade from basal granule to medium sand conglomerate or grainstone to medium–fine sand wackestone at the top. Two of these units show distinct parallel stratification, whereas the two others are somewhat homogenised by burrowing. One of the units consists of well-defined rounded chalk clasts, whereas the others are mainly composed of highly compressed chalk clasts with diffuse boundaries, and numerous holes after dissolved grains. The chalk clasts commonly appear to be welded together and may be deformed by burrows or at grain–grain contacts. A spectacular example is provided by a 25 cm thick graded, coarse pebble to granule conglomerate bed composed entirely of chalk clasts (Fig. 23). A texturally similar unit occurring between two Facies 14 units shows heavily deformed boundaries.

Interpretation. The diagnostic character of Facies 11 is the dominance of chalk clasts. It can be envisaged that significant numbers of relatively large chalk clasts may be produced by erosion and reworking of firm, buried chalk or of early diagenetic chalk nodules. Liberation of the relatively large numbers of chalk clasts making up the conglomerates and grainstones of Facies 11, however, would have required reworking of large volumes of chalk, and subsequent segregation of the mud and sand-to-pebble fractions. Winnowing of ooze from nodular chalk or from a chalk debrite could produce a lag conglomerate composed entirely of chalk clasts. The winnowing process would have involved removal

1 cm

Fig. 23. Exceptional example of a graded, clast-supported chalk conglomerate (Facies 11; 3269.21–3268.95 m, see Plate 1). Intergrain pore space is filled with cement and is largely devoid of mud.

A

B

1 cm

C

1 cm
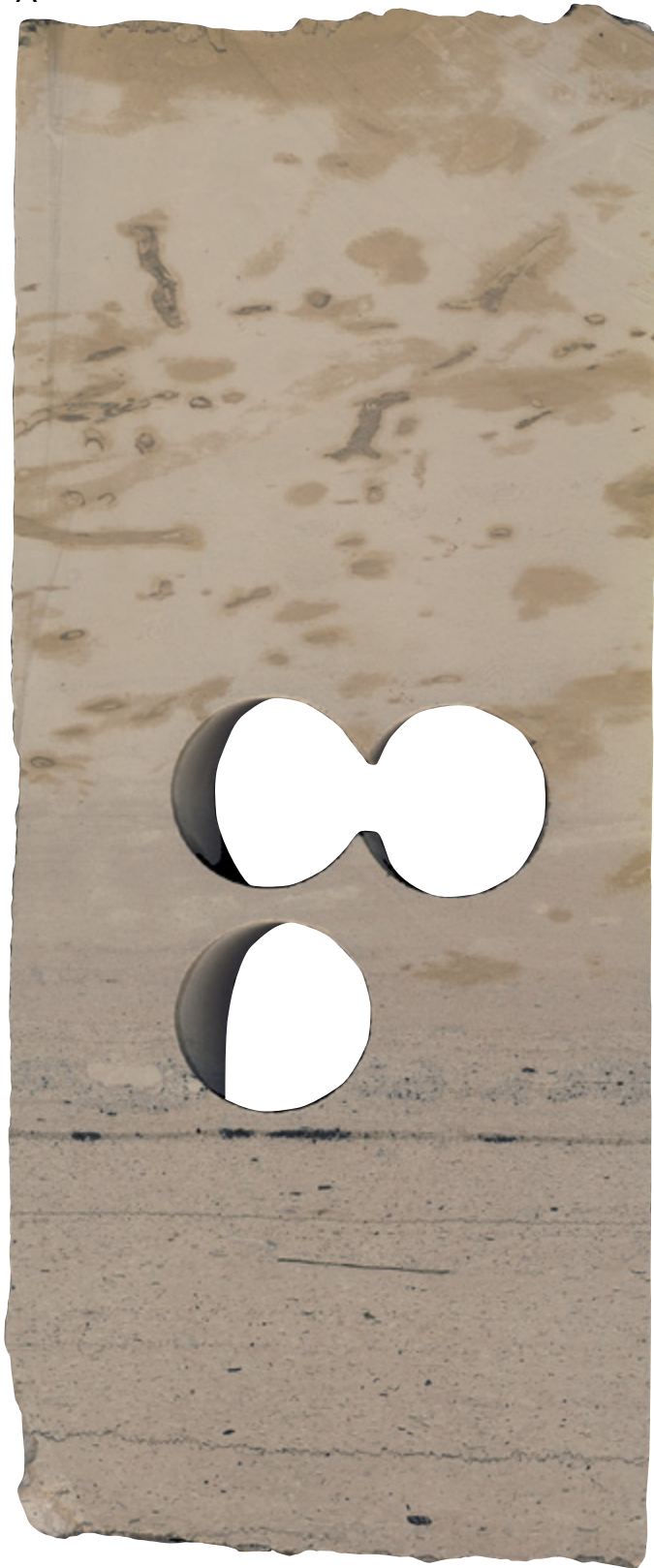
1 cm

Fig. 25. Downstream maturation of debris flows whereby mud is progressively expelled from the flow until it consists of an upper mudflow and a basal turbidity/grain flow. Inspired by Krause & Oldershaw (1979).
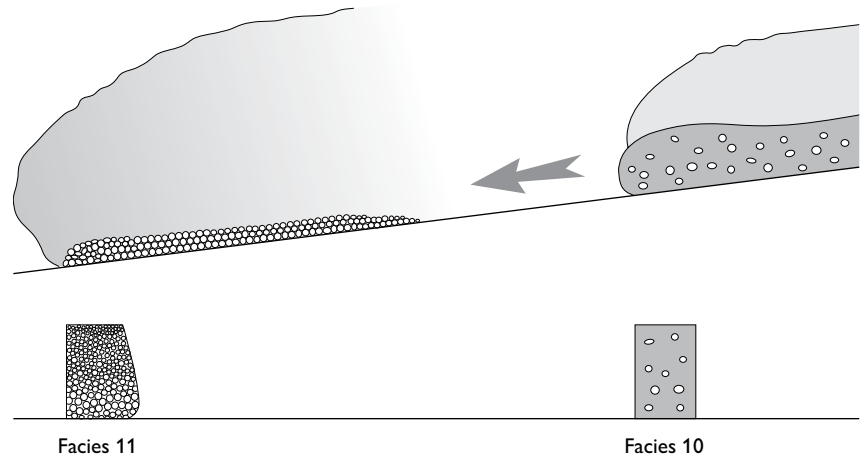
of enormous amounts of chalk ooze to produce conglomerates of the thicknesses observed in the Mona-1 core. It would take numerous cycles of debris flow or nodular hardening followed by complete removal of mud to produce thick layers of conglomerate or grainstone, because a thin residual lag would form an armoured layer sheltering the underlying chalk. Furthermore, the lag would have to be reworked after its formation to produce the grading observed in Facies 11. A more likely explanation is that the loss of mud occurred by extreme down-slope maturation of debris flows, whereby mud was expulsed from the flows (see Krause & Oldershaw 1979), until the point where the debris flows had essentially evolved into concentrated density flows as indicated by the overall normal grading of most units (Fig. 25). Grain flow dynamics affected the basal part of some flows during the final stages of deposition as indicated by the presence of basal inverse grading.

Facing page:
Fig. 24. Clast-supported chalk conglomerates and pebbly grainstones (Facies 11); all samples are largely composed of chalk clasts. **A**: Normally graded and laminated grainstone mainly composed of coarse–fine sand-grade chalk clasts with some scattered chalk granules and pebbles (3343.93–3343.68 m, see Plate 1). **B**: Deformed conglomerate with clasts up to 5 cm across (3275.57–3275.41 m, see Plate 1). **C**: Conglomerate (3361.79–3361.94 m, see Plate 1); somewhat contorted due to compaction, but the overall grading is retained. The black colour is due to pyrite.
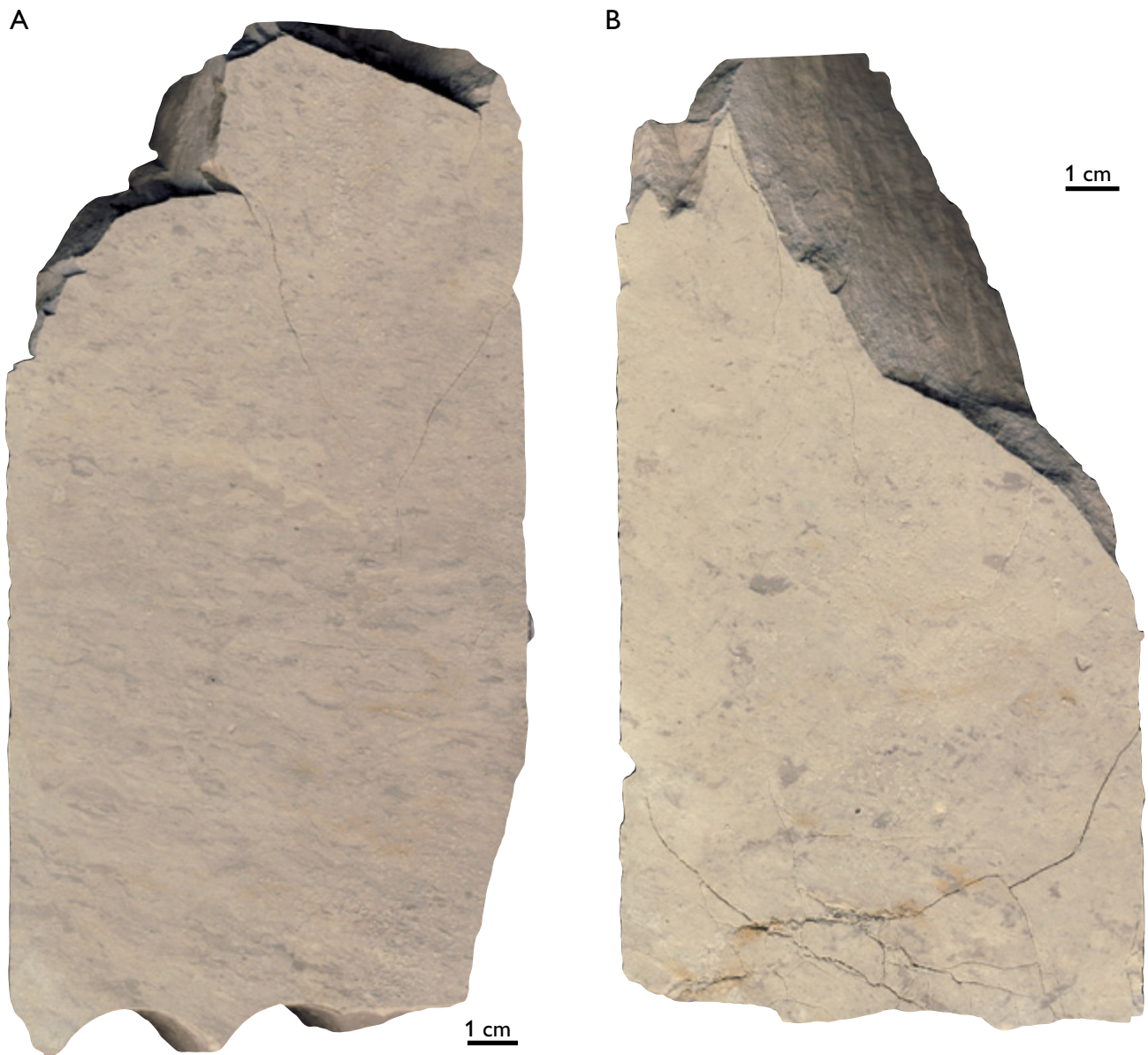
Fig. 26. Shear-deformed bioturbated chalk (Facies 12; **A**: 3183.03–3182.85 m. **B**: 3159.99–3159.86 m, see Plate 1). Note the mottled fabric, which appears to have been slightly deformed.

Facies 12: Shear-deformed bioturbated chalk

Description. This facies may be regarded as a variant of Facies 1, but it is described separately as it is important for the understanding of the mass-transport processes and the porosity variations. It is characterised by its generally biomottled but shear-deformed fabric (Fig. 26). The biomottled fabric is evident but individual burrows are poorly preserved. *Planolites* and *Chondrites* can commonly be recognised by their morphology and configuration, but their margins show stepwise lateral off-sets on the submillimetre scale. Well-defined shear zones, several centimetres thick, showing larger strain than the remaining unit have only been observed at the base of one unit. Deformation was thus accommodated

Fig. 27. Photomicrographs of thin section of shear-deformed bioturbated chalk (Facies 12; 3182.39 m, see Plate 1) seen in plane polarised, transmitted light (**A**) and under-crossed polars (**B**). Note the absence of intraparticle cement and thus preservation of porosity.
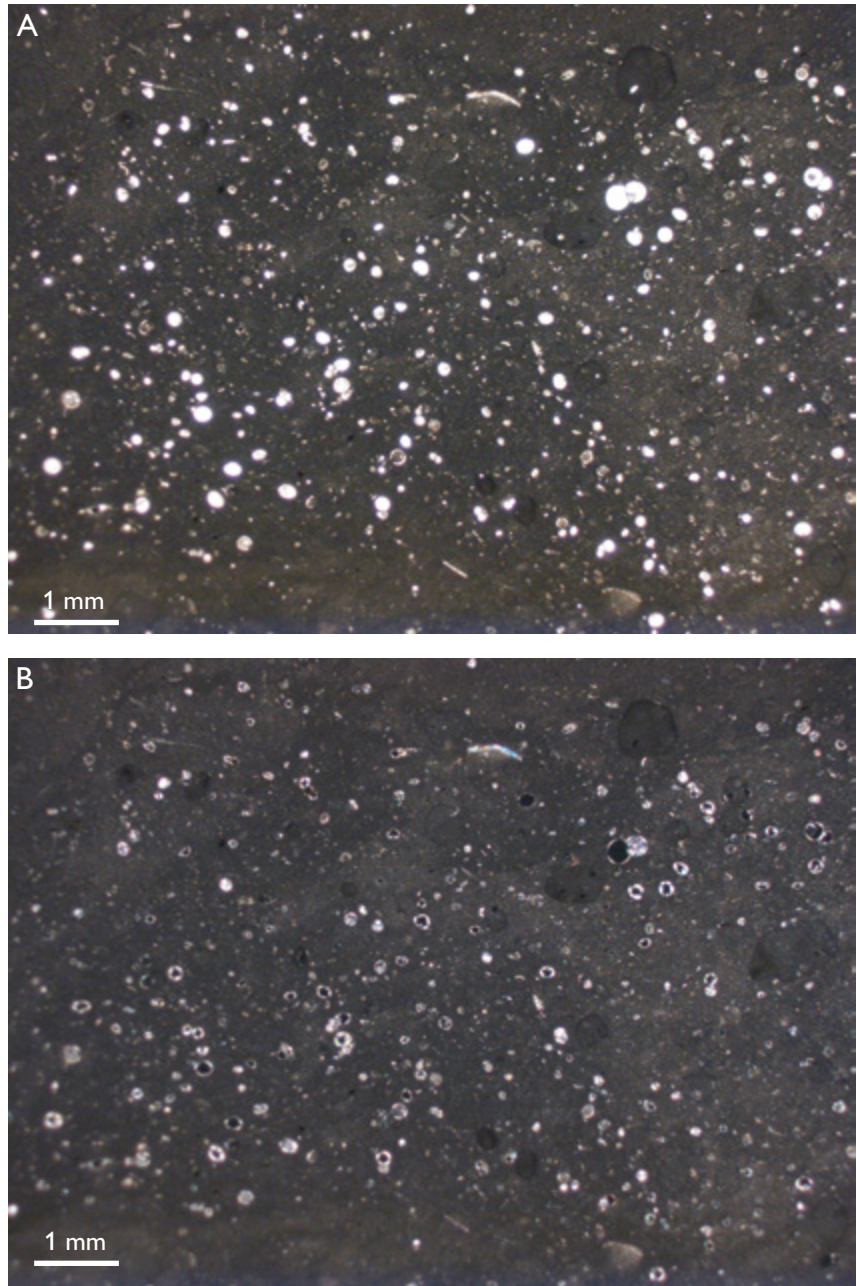
by limited displacement along numerous submillimetre-scale shear zones distributed rather evenly throughout the units. The amount of displacement along each of the small-scale shear zones may vary gradually within units. Thus, undeformed bioturbated chalk (Facies 1) may grade upwards into shear-deformed bioturbated chalk (Facies 12), showing gradually increasing strain upwards to the point where the bioturbated fabric is hardly recognisable. Units showing relatively large strain commonly contain small sand to granule grade intraclasts formed by the shearing. Slightly more con-

solidated parts of the chalk apparently remained coherent during shearing of the surrounding chalk and hence produced undeformed but slightly displaced and sharp-bounded intraclasts. There thus appears to be a gradual transition between Facies 12 and Facies 14 with relatively few and small intraclasts, and these two facies are difficult to distinguish in the uppermost part of the core.

There are nine individual occurrences of the facies in the core. The units are 25–660 cm thick and make up a total of 17.2 m. They are restricted to mass-transport

intervals and are typically associated with Facies 13 and 14. The boundaries to other facies can only be observed in a few cases due to stylolites and because the facies is mostly found in highly porous parts (Fig. 27), where the core condition is relatively poor. However, it appears that the facies may have either sharp or gradational boundaries to other facies.

Interpretation. Facies 12 represents small-scale plastic deformation of bioturbated chalk. The deformation may have occurred through several different processes. A common problem of core interpretation is to determine whether units occur in place between two slump units or they represent transported units within a single slump. The four upper Facies 12 units almost certainly represent deformed bioturbated chalk within larger slumps, and are thus allochthonous, whereas the two lower Facies 12 units were probably formed by deformation of bioturbated chalk by overriding debris flows, and therefore essentially represent in-place deformation (Plate 1). One unit at 3274.2 m (10 743 ft) probably represents limited lateral creep of bioturbated chalk. Two thin units, at 3218.4 m (10 559 ft) and 3182.7 m (10 442 ft), may be interpreted as bioturbated chalk deformed by overriding debris flows or slumps, or alternatively as intra-slump units. It is important to note that intraclasts may form through shear deformation of consolidated chalk.

Facies 13: Shear-deformed matrix-supported chalk conglomerate

Description. This facies shares most of the general characteristics of Facies 10, but differs in showing shear-deformation structures and in having a heterogeneous clast distribution (Figs 28, 29). The deformation structures are seen as irregular colour bands in the matrix, which define open to tight subangular folds. Several orders of smaller folds are superimposed upon larger folds and the boundaries between individual colour bands appear somewhat serrated and show small-scale flame structures. Evidence for shear deformation on clast margins is relatively common and some clasts are sheared to the point at which they form thin white bands. Clasts are randomly distributed on a decimetre scale, but are rather unevenly distributed on a larger scale, which may be due to larger-scale folding. There are 27 oc-

currences of the facies, which makes up a total of 50 m of the core. Individual units are 20–960 cm thick and almost exclusively associated with mass-transport facies. Most commonly, Facies 13 shows gradual transitions to other shear-deformed facies (Facies 12, 14 or Facies 9 with deformation structures), and gradational transitions to Facies 14 are particularly common (Fig. 30). More rarely, the facies has rather sharp boundaries, which may be marked by a thin shear zone or bedding discordances.

Interpretation. This facies represents debrites deformed either by slumping or due to shearing by overriding flows or slumps. The precursor facies was similar to Facies 10, but was plastically shear-deformed. The shear deformation most commonly occurred within larger-scale deformed units, involving several different facies. It is difficult to determine whether stacks of shear-deformed facies represent single or multiple deformation events, especially in a core. In the 3422.7– 3415.6 m (11 229 ft 4 in. – 11 206 ft) interval, the facies definitely represents three events as shown by burrowed surfaces within the succession. Individual event beds were only a little more than 1 m to less than 4 m thick. In the lowermost bed, the degree of shear deformation increases upwards so that Facies 10 grades into Facies 13. In most cases, the deformation appears to have occurred subsequent to deposition, but it cannot be ruled out that some of the thin slumps composed of only Facies 13, or Facies 10 and 13 together, were deformed during the final stages of debris flow as the rheology of the material entered the plastic phase. In that case, the shear deformation was driven by the inertia of the debris flow itself, rather than by later additional gravity-induced stress.

Fig. 28. Typical shear-deformed, matrix-supported chalk conglomerate (Facies 13; 3197.44–3197.28 m, see Plate 1). The facies appears similar to Facies 10, but shows evidence for shear-deformation through relatively gentle folding.
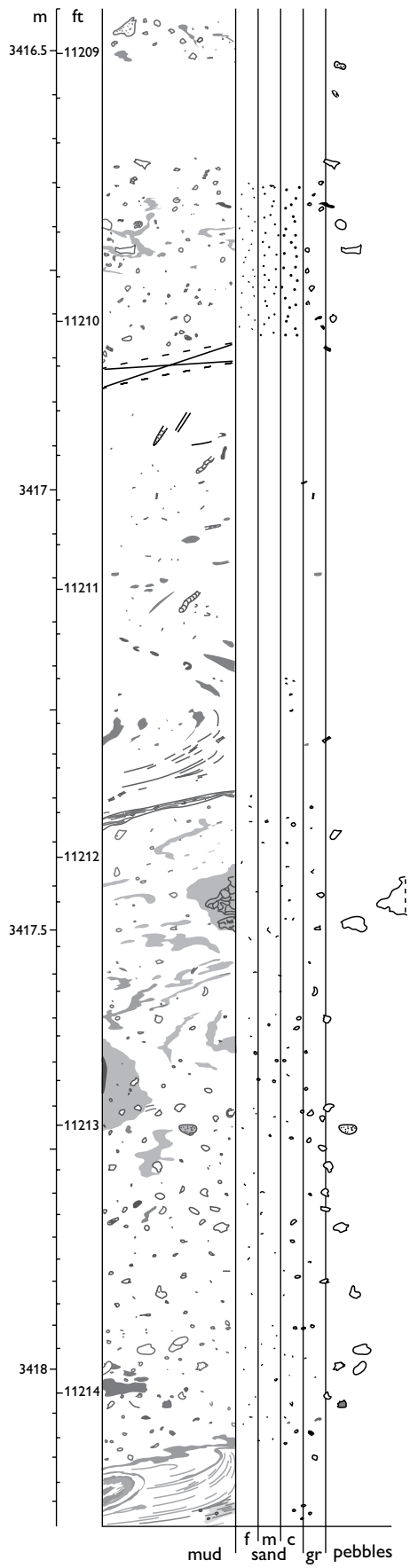
Fig. 29. Typical shear-deformed, matrix-supported chalk conglomerate (Facies 13, see Plate 1) succession with evidence for both metre- and centimetre-scale folding and a random clast distribution.

Chalk clasts and shell fragments

Colour banding

Burrows

Missing core
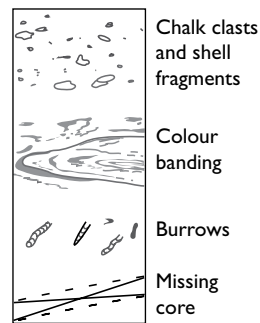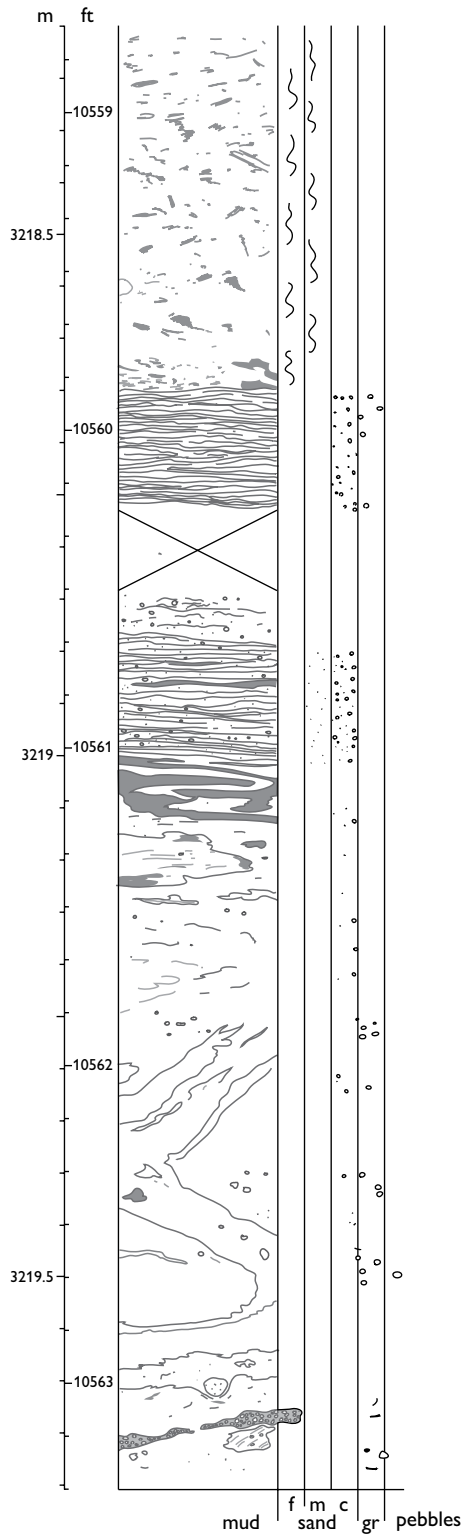
Fig. 30. Succession showing a gradual upward transition from shear-deformed, matrix-supported chalk conglomerate to shear-banded chalk (Facies 13–14). The transition at *c.* 3219 m is defined by a gradual, upward-increasing aspect ratio of folds with the boundary between Facies 13 and 14 at 3219 m. The top part is bioturbated chalk (Facies 1).
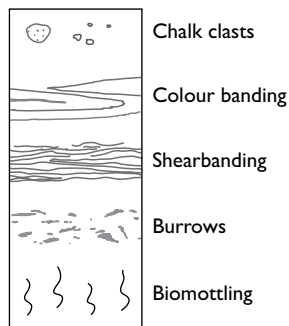
Fig. 31. Shear-banded chalk (Facies 14; 3344.41–3344.22 m, see Plate 1) with relatively small, rounded chalk clasts. The colour banding shows the limbs of small isoclinal folds in the lower half of the sample.

Facies 14: Shear-banded chalk

Description. This facies is characterised by the presence of matrix-supported chalk clasts, as in Facies 10 and 13, but differs in showing an irregular colour banding (Figs 31, 32, 33). The bands are 2–20 mm thick, and most are around 8 mm thick. Individual bands are slightly wavy with somewhat irregular thickness. Their boundaries have a skewed, serrated or flame-like appearance similar to those of Facies 13. The bands commonly form thin recumbent isoclinal folds with closely spaced limbs, and the bands may also form larger, more open folds, especially when transitional to Facies 13. The concentration of clasts varies greatly, both within and between individual units. They appear to show a random distribution within units and are mostly medium sand- to granule-sized. Larger clasts occur less commonly than in Facies 10 and 13, and some units contain very few clasts. Larger clasts commonly protrude through both base and top of single colour bands, but it is equally common to see colour bands that envelop clasts larger than the thickness of the band. Some units contain distinct sandy layers up to a few centimetres thick, which have the same irregular appearance as the colour bands (Fig. 33). It is difficult to distinguish units of Facies 14 that have a low colour contrast and very few clasts from the most deformed units of Facies 12.

Facies 14 is very common and makes up a total of 56 m distributed over 25 individual units, which are 15–705 cm thick. The facies is closely associated with Facies 12 and 13. Lower boundaries are either gradational to Facies 13 or sharp and in some cases sheared into various other facies. Upper boundaries are mostly gradational to slightly deformed Facies 9 or Facies 12 and 13, or sharp and in some cases discordant to Facies 6, 9, 12, or 13.

Interpretation. This facies was formed through intense plastic shear deformation of chalk. The chalk must have been in an unlithified but somewhat dewatered and firm state, indicating a burial depth of about 10–200 m prior to deformation (Mallon & Swarbrick 2002). The close and gradational association with the folded Facies 13 and the many examples of thin recumbent isoclinal folds indicate that the laminated appearance of the matrix is a type of shear banding. Relatively gentle shear folding of firm but non-hardened chalk produced Facies 13, whereas further shear deformation produced more folds and stretched already existing folds. This process caused a gradual horizontal lengthening and

vertical shortening of the recumbent folds, and thus a higher aspect ratio. A core section through a succession of very thin recumbent folds with very large aspect ratios would display numerous beds or laminae, representing the limbs and only few fold hinges. It is quite possible that the process proceeded beyond the point of dismemberment at the fold hinges, thus further diminishing the likelihood of encountering a hinge in a core section. Similar structures have been referred to as 'shredded' and have been attributed to 'secondary shear-induced lamination' in relation to slumping (Kennedy 1980) and 'flow-induced lamination', which may form during the final stages of debris flows (Nygaard *et al.* 1983). The lamination is clearly a product of plastic deformation and it is difficult to determine if the deformation within a debrite occurred during the final stages or after deposition of a fluidal debris flow. However, as with Facies 13, it appears likely that debris flows entered a phase of plastic rheology during their final stages of flow, as also suggested in the interpretation by Nygaard *et al.* (1983).

The close association between Facies 10, 13 and 14 indicates that Facies 14 was typically produced by shear deformation of debrites (Facies 10 and 13). However, Facies 14 may also be produced by shear deformation of several other facies. Units of Facies 14 typically contain fewer and on average smaller chalk clasts than Facies 10 and 13, mainly due to destruction of the clasts during intense shearing. It is also evident that chalk clasts may be produced directly by shear deformation of bioturbated chalk, as seen in Facies 12, and a similar process may be expected to have occurred during the formation of Facies 14. In that case, the 'clasts' are products of largely in-place brecciation of soft but firm chalk rather than true transported clasts. It is not possible to confidently distinguish the two in the present case, and the term clast is therefore maintained for simplicity. The distinction between Facies 12 and 14 is often quite subtle, especially in the upper part of the core. In this interval, the similarity between relatively strongly sheared and clast-bearing Facies 12 and 14 with weakly developed colour banding, suggest that the two facies are part of a continuum. In two other cases, at 3426.4 m (11 241 ft 7 in.) and 3218.1 m (10 558 ft 2 in.), Facies 14 contains numerous deformed bioclastic sandy layers and appears to have been produced by deformation of a Facies 1–8 dominated succession (Fig. 33).

Fig. 32. Examples of shear-banded chalk (Facies 14; **A**: 3257.02–3256.79 m. **B**: 3307.94–3307.84 m. **C**: 3325.22–3325.08 m, see Plate 1). **A** shows relatively regular colour bands, whereas **B** and **C** show contorted, irregular colour bands.
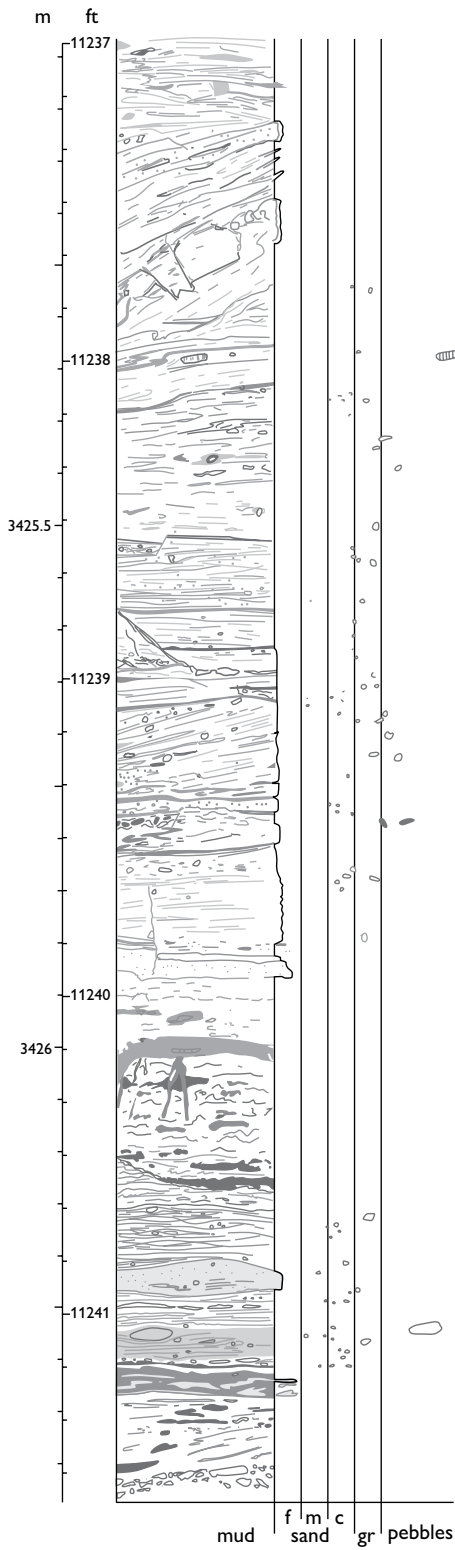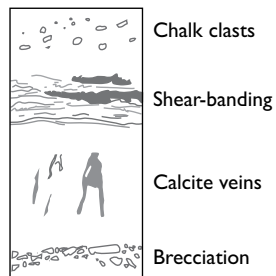
Fig. 33. Log example of shear-banded chalk (Facies 14) containing deformed sandy layers, suggesting that it was formed by shear deformation of a pelagic/turbiditic succession (Facies 1–8).

Chalk clasts

Shear-banding

Calcite veins

Brecciation

m ft

11237

11238

3425.5

11239

11240

3426

11241

mud   f m c
       sand   gr pebbles

Slumps

All the facies described above may have been incorporated into a slide or slump, yet none of the facies are diagnostic of slides and slumps. The recognition of slides and slumps must therefore be based on other parameters than facies alone. Slides, defined as lateral transport of sediment along discrete shear planes with little or no internal deformation (e.g. Stow *et al*. 1996), are difficult to recognise in cores. Slumps are more easily recognised because they are internally deformed (Stow *et al*. 1996), but it is often difficult to determine the number of depositional events represented by a succession of slumped facies. Shear zones and undeformed burrow horizons may define the base and top of slumps, but even these criteria must be cautiously applied. Apparently 'normal' burrowed/bioturbated chalk may represent undeformed but redeposited boulders, and shear zones may develop internally within slumps so that they do not define the base of a depositional unit. Bypassing debris flows and slumps may cause deformation of the underlying strata, producing similar structures to those formed in a slump. This type of deformation did not involve subaqueous motion of the deformed sediment and should be distinguished from true slides and slumps.

Fourteen intervals (numbered S1–S14 in ascending stratigraphic order) are interpreted to represent slumps (Table 2). Several of these contain thin zones of undeformed bioturbated chalk. In S14, the undeformed zones appear to be overturned, judging from the general alignment of the biomottled fabric and the bifurcation direction of *Chondrites*. In S12, a slightly deformed bioturbated zone is sharply based, which would not be the case if it represented the bioturbated top of a slump. Overturned and sharply based bioturbated zones represent undeformed boulders or plugs within slumps rather than the burrowed top of a slump. In other cases, the zones appear to be correctly oriented and the boundaries are not preserved or marked by stylolites. Such zones may represent pelagic deposition between slump events or undeformed boulders. S6, S7, S10 may represent multiple events, and there are thus 14–18 slump events represented in the succession, and individual slump units are 2 m to more than 42 m thick.

Debrites appear to be the most common precursor facies involved in slumping and there are several possible explanations for this. The slump structures may have formed during the transition between fluid and plastic behaviour as an integral part of debris flow deposition. Slumps and debris flows probably developed due to similar preconditions and triggers, meaning that they occur in the same temporal and spatial setting. Debrites lacked the efficient dewatering of more slowly deposited and bioturbated sediment, and were therefore more susceptible to renewed slope failure.

Table 2. Slump units: distribution and characteristics

	Depth	Thickness	Facies	Precursor facies	Remarks
S1	3426.56–3424.17 m (11242 ft–1234 ft 2 in.)	2.39 m	14	Pelagite/ turbidite succession	Highly shear-deformed chalk with few and small chalk clasts and deformed sandy packstone layers. Burrowed at top.
S2	3422.70–3420.52 m (11229 ft 4 in.–11222 ft 2 in.)	2.18 m	13 10	Debrite	Debrite shear-deformed on the sea floor (slump) or in the subsurface by subsequent debris flow. Capped by turbidite.
S3	3420.52–3415.39 m (11222 ft 2 in.–11205 ft 4 in.)	5.13 m	13	Debrite	Basal shear surface and burrows at top. Succeeded by four amalgamated mudflow units (Facies 9).
S4	3398.14–3390.52 m (11148 ft 9 in.–11123 ft 9 in.)	7.62 m	14 13	Pelagite?	Highly shear-deformed slump with few and relatively small chalk clasts, suggesting a non-debrite origin. Internal zone of less pronounced deformation (Facies 13).
S5	3382.90–3378.63 m (11098 ft 9 in.–11084 ft 9 in.)	4.27 m	14 13	Debrite	Basal shear zone.
S6	3323.52–3317.14 m (10910 ft 6 in.–10883 ft)	8.38 m	13 12 14	Lower half probably pelagite, upper part debrite	One or two slump events. Possibly one large slump with internal zone/boulders of bioturbated chalk, or three discrete slumps separated by pelagic deposits.
S7	3314.85–3307.69 m (10875 ft 6 in.–10852 ft)	7.16 m	14 13 1 10	Debrite	Facies 1 unit appears to be inverted suggesting it is a large clast within a large slump. If not, the unit separates two discrete flow units.
S8	3307.08–3302.81 m (10850 ft–10836 ft)	4.27 m	13 14	Pelagite	Basal part of unit was probably originally a debrite. Capped by turbidite.
S9	3282.39–3275.69 m (10769 ft–10747 ft)	6.70 m	13 14 9	Debrite/ pelagite succession	Basal shear zone. Capped by turbidite.
S10	3275.46–3272.64 m (10746 ft 3 in.–10737 ft)	2.82 m	1 13 14 3	Pelagite	Bioturbated interval (Facies 1) may represent pelagic deposition between two slump events, or an undeformed plug or boulder within a single slump.
S11	3257.09–3250.01 m (10686 ft–10662 ft 9 in.)	7.08 m	14	Debrite	
S12	3227.43–3216.81 m (10588 ft 8 in.–10553 ft 10 in.)	10.62 m	14 13 12 10	Debrite/ pelagite/ turbidite succession	Highly shear-deformed succession. Originally basal debrite and upper pelagic/turbidite interval. Facies 12 interval shows sharp lower boundary, indicating that it represents a boulder within the slump.
S13	3202-23–3188.00 m (10506 ft–10459 ft 4 in.)	14.23 m	13 14	Debrite	
S14	3184.70–3142.49 m (min.) (10448 ft 6 in.–10310 ft)	>42.21 m	12 14 13 1 10	Pelagite/ debrite succession	Bioturbated chalk intervals are overturned. Several internal discordant surfaces.

Genetically related facies

Facies 1–4 (Table 1) are all interpreted to be the product of pelagic deposition, possibly interrupted by deposition of thin event beds, and are collectively termed pelagites. Facies 5–8 and Facies 11 are all interpreted as having been deposited by turbidity flows and are collectively termed turbidites. Facies 7 and 8 are interpreted as equivalent to the basal part of Facies 6, and Facies 5 is equivalent to the uppermost part of Facies 6. Facies 7 and 8 thus, in theory, represent the most high-energy (or proximal) turbidites and Facies 5 the most low-energy (or distal) turbidites (Fig. 34). Facies 2 (laminated chalk) may be incorporated into this scheme as representing the most distal or low-energy facies related to turbidity flows. Facies 11 was produced by down-slope evolution of debris flows (Fig. 25). Limited shear deformation produced distinctly deformed facies from which the precursor facies can still be deduced (Facies 12 and 13), whereas intense or continued shear deformation produced the shear-banded Facies 14 from which the precursor facies cannot be deduced in all cases. Facies 9, 10 and all beds occurring within the 14 slump units were deposited by mass transport as defined by Moscardelli & Wood (2008) and are collectively termed mass-transport deposits.
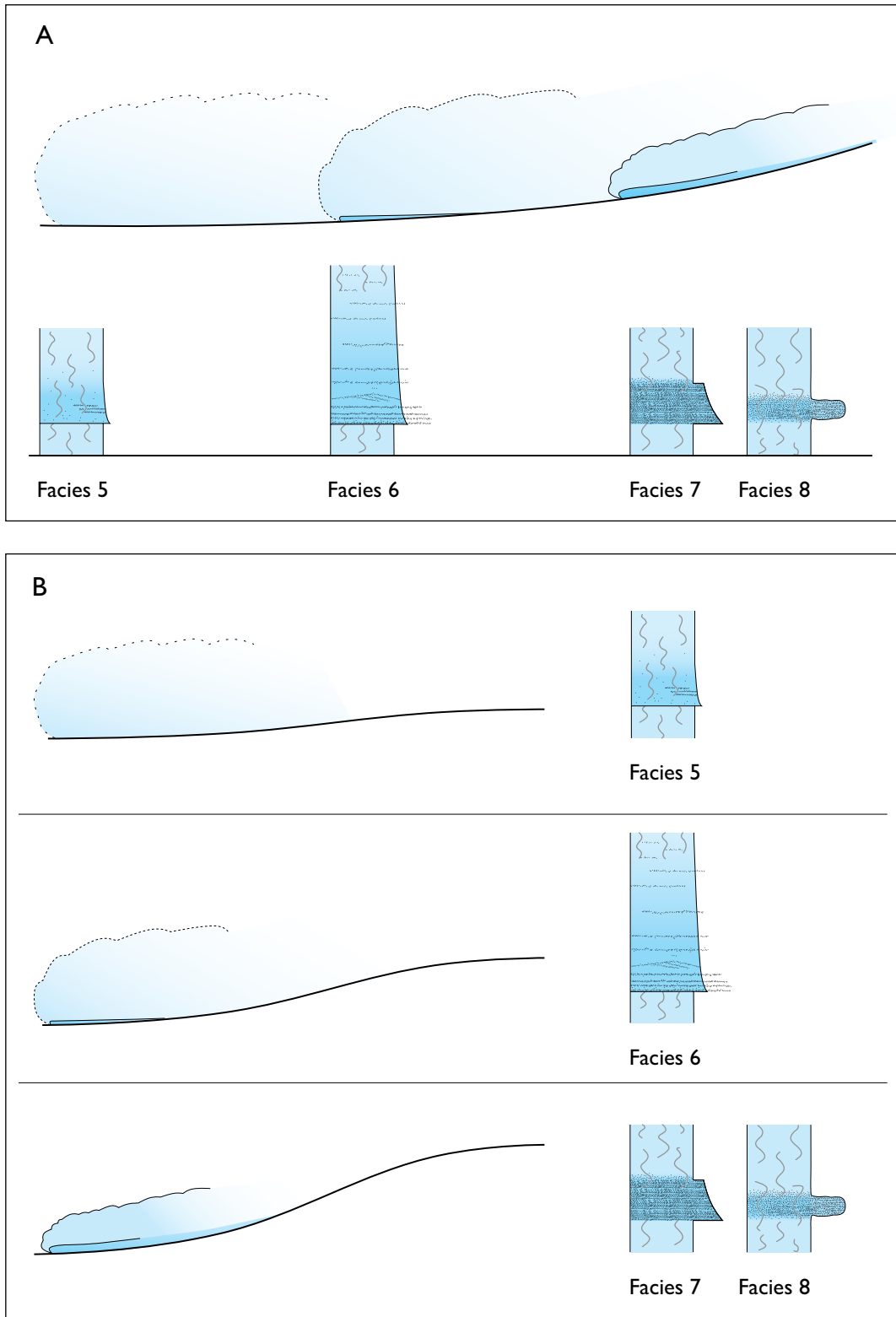
Fig. 34. Hypothetical relationship between turbidite Facies 5–8, interpreted to represent distance to source area (**A**) or variable basin gradients (**B**).

Facies associations and stratigraphic development

Facies associations

Three facies associations are defined on the basis of a dominant or characteristic group of facies. They comprise intervals dominated by pelagic deposits, mixed pelagite/turbidite intervals, and intervals dominated by mass-transport deposits.

Facies association 1 (pelagic chalk)

Description. Facies association 1 (FA 1) occurs in six intervals and makes up 26% of the Upper Cretaceous succession (Fig. 35, Plate 1). It is dominated by pelagic facies, mainly Facies 1 with subordinate Facies 2–4. Intrapelagic erosion surfaces are common in the lower part of the core and turbidites are rare and occur dispersed through the pelagic intervals. Mass-transport facies are very rare, and there appears to be no systematic ordering of facies within intervals belonging to this facies association.

Interpretation. FA 1 represents prolonged periods of relatively stable pelagic deposition, only rarely interrupted by redepositional or erosional events caused by bottom currents or benthic storms. Although the association accumulated mainly under well-oxygenated benthic conditions, dysoxic bottom conditions occurred periodically. The rarity of redeposited facies indicates tectonic quiescence and a low-gradient basin topography.

Facies association 2 (turbiditic chalk)

Description. Facies association 2 (FA 2) occurs in two intervals and makes up 23% of the Upper Cretaceous succession (Fig. 35, Plate 1). It is represented by common to abundant turbidites, alternating with pelagites and rare to common mass-transport facies. Bioturbated chalk (Facies 1) is the most common pelagite, but laminated chalk (Facies 3) dominates in the lowermost part of the lower interval and occurs locally throughout both intervals. Intrapelagic erosion surfaces are common in

the upper part of the upper interval. Turbidites show an overall thinning-upward development, but shorter subintervals may show either thinning- or thickening-upward trends. The dominant turbidite facies changes upwards from Facies 6 to Facies 7, to Facies 8 and finally to Facies 5 (Fig. 36).

Interpretation. FA 2 represents a relatively dynamic depositional environment with pelagic deposition interrupted by recurring slumps, turbidity, mud and debris flows. Benthic dysoxia occurred episodically, but most of the facies association accumulated under well-oxygenated benthic conditions. The association is interpreted to represent deposition in a basinal setting.

Facies association 3 (mass-transport chalk)

Description. Facies association 3 (FA 3) occurs in six intervals and makes up 51% of the Upper Cretaceous succession (Fig. 35, Plate 1). It is overwhelmingly dominated by mass-transport facies with only a few occurrences of non-reworked pelagites and turbidites. Deformed facies and debrites constitute most of FA 3, and most of the facies occur in inferred slumps. A systematic ordering of facies is not observed within intervals belonging to FA 3.

Interpretation. FA 3 represents debris flow, mudflow and intervening pelagic deposition, and all of the resultant facies were commonly reworked into slumps. The association is interpreted to represent relatively unstable periods of the depositional history.

Facing page:
Fig. 35. Simplified log of the studied succession showing the distribution of facies associations and the subdivision into stratigraphic intervals **a–e** discussed in the text. **Alb.**: Albian. **Cen.**: Cenomanian. **Camp.**: Campanian.

Depth
m   ft

Facies association | Description | Interpretation

FA 3

3184.70 m
(10448 ft 6 in.)   FA 1

3191.05 m
(10469 ft 4 in.)   FA 3

3202.23 m
(10506 ft)   FA 1

3216.81 m
(10553 ft 10 in.)

FA 3

Dominated by mass-transport deposits alternating with pelagites. Turbidites are very rare and deformed facies become increasingly dominant and thicker upwards.

Pelagic deposition interrupted by increasingly large and frequent mass-transport events.

3257.09 m
(10686 ft)   FA 1

3272.64 m
(10737 ft)   FA 3

3282.39 m
(10769 ft)   FA 1

3290.77 m
(10796 ft 6 in.)   FA 2

3301.70 m
(10832 ft 4 in.)

FA 3

3324.10 m
(10905 ft 10 in.)

FA 1 | Pelagites with some intrapelagic erosion surfaces, turbidites and thin debrites. | Relatively quiet deposition in a low-gradient basin.

3352.11 m
(10997 ft 9 in.)

FA 2 | Pelagites alternating with common turbidites and some mass-transport deposits. Turbidites show an overall thinning-upward trend and an upward change from dominantly high-energy to low-energy turbidite facies; individual intervals bounded by mass-transport facies commonly show opposite trends. | Deposition of prograding and aggrading intervals during gradually decreasing basin gradients.

3411.55 m
(11192 ft 9 in.)

FA 3 | Dominated by debrites, mud flow deposits, and deformed facies. Also minor pelagites and turbidites. | At least eight discrete mass-transport events, probably due to uplift of the Mona Ridge.

3440.58 m
(11288 ft)

FA 1 | Upward transition from laminated marl to bioturbated marly chalk. | Hemipelagic/pelagic deposition. Increasing oxygenation and reduced influx of siliciclastic material.

upper Maastrichtian
lower Maastrichtian
upper Camp.
*
Cen.
upper Alb.

* middle Coniacian – lower Santonian

Legend:
Pelagic chalk
Turbiditic chalk
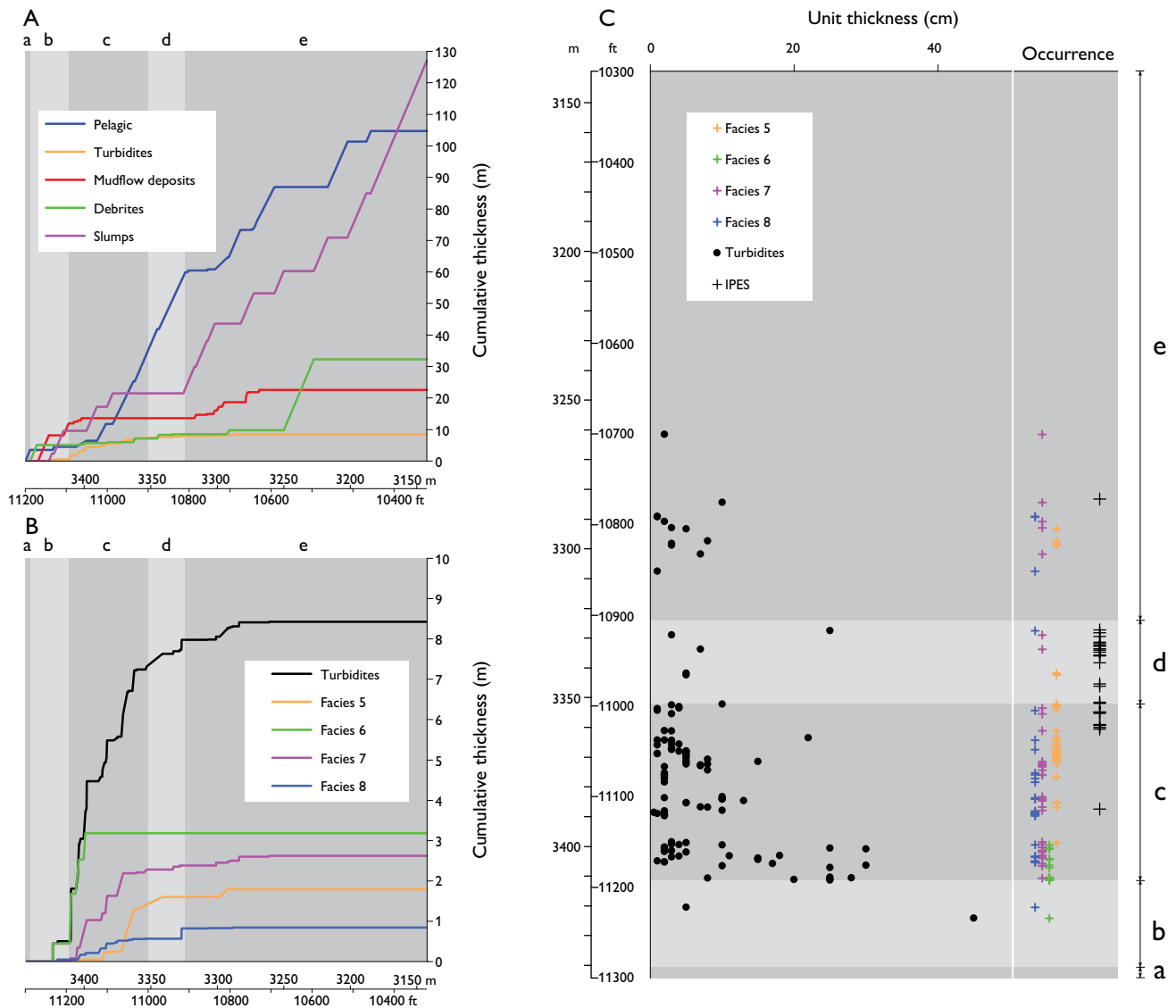Mass-transport chalk

e
d
c
b
a

Fig. 36. **A**: Cumulative thickness of pelagites, turbidites, mudflow deposits, debrites and slumps. Note the upward change from mixed deposits to pelagite-dominated deposits and to slump-dominated deposits with intervening pelagites. Debrites are under-represented in this plot as they were typically incorporated into slumps. **B**: Cumulative thickness of turbidites. Note the upward change in the dominant facies from Facies 6 through 7 and 8 to 5. This suggests a prograding to aggrading basin development, but note that according to Bailey *et al.* (1999) this interval spans a considerable hiatus (compare with Figs 34, 37). **C**: Thickness of turbidites (left panel) and occurrences of individual turbidite facies and intrapelagic erosion surfaces (IPES) (right panel). The plot illustrates the overall upward decreasing importance of turbidites, and the right panel shows that the upward change in dominant facies illustrated in **B** is succeeded by an increase in the occurrence of intrapelagic erosion surfaces. Stratigraphic intervals **a–e** from Fig. 35

Stratigraphic development

The succession belongs to the Upper Cretaceous with the exception of the lowermost 1.8 m (Bailey *et al.* 1999) (Fig. 35, Table 3). The cored section extends up-wards to 9.73 m below the Cretaceous–Tertiary boundary, which is reported to occur at 3132.7 m (10 278 ft) (Bailey *et al.* 1999). The biostratigraphical zonation defined by Bailey *et al.* (1999) was calibrated to the chronostratigraphic scheme of Ogg *et al.* (2004). More

Chronostratigraphy	Depth	Age (Ma)

Table 3. Chronostratigraphic subdivision*

Chronostratigraphy	Depth	Age (Ma)
	3132.73 m (10278 ft)	65.5
upper Maastrichtian (UC20)†		
	3288.79 m (10790 ft)	68.6
upper Maastrichtian (UC19)		
	3332.23 m (10932 ft 6 in.)	69.2
lower Maastrichtian (UC18)		
	3386.56 m (11110 ft 9 in.)	70.4
upper Campanian – lower Maastrichtian (UC17)		
	3416.20 m (11110 ft 9 in.)	75.2
upper Campanian (UC16)		
	3386.56 m (11208 ft)	75.8
lower Santonian – upper Campanian (UC12–15)		
	3416.20 m (11208 ft)	84.5
middle Coniacian – lower Santonian (UC10–11)		
	3426.56 m (11242 ft)	88.0
Turonian – middle Coniacian		
	3426.56 m (11242 ft)	93.5
Cenomanian		
	3444.09 m (11299 ft 6 in.)	99.6

*Subdivision based on the biostratigraphic analysis of Bailey et al. (1999) with the addition of chronometric ages from Ogg et al. (2004)
†UC = Upper Cretaceous nannofossil zones from Burnett (1998)

than half of the time represented by the studied succession is represented by hiatuses, and little more than 10% of the time is represented by pelagic deposits (Fig. 37). The pelagic intervals show common signs of erosion and the remaining succession is composed of event deposits, which can be considered to have formed geologically instantaneously. This implies that 90% of the Late Cretaceous Epoch is not represented in the succession. There is, however, great uncertainty involved in applying biostratigraphical markers within a succession that is strongly influenced by redeposition. Based on the available data, however, the succession is subdivided into five intervals (a–e on Figs 35–37, 39):

(a) The lower 5.5 m of the succession (3446.1–3440.6 m, 11 306 ft – 11 288 ft) belongs to FA 1 and is of latest Albian – Cenomanian age (Fig. 35). The interval shows an upward transition from laminated marl (Facies 4) to bioturbated marly chalk (Facies 2), which is interpreted to represent increased benthic oxygenation, enhanced production of pelagic carbonate and reduced siliciclastic influx.

(b) This is succeeded by a 29 m thick interval (3440.6–3411.6 m, 11 288 ft – 11 192 ft 9 in.) belonging to FA 3 and referred to the Cenomanian – late Campanian age range. It represents at least

eight individual mass-transport events, including a debrite with boulders of the older marly chalk in a matrix derived from relatively shallow-water carbonates, as well as two turbidites and minor intervening pelagites. This interval is interpreted to represent significant tectonic activity and uplift of the Mona Ridge. Non-deposition or erosion thus characterised the Cenomanian – late Campanian interval, only interrupted by mass-transport events (Fig. 38A, B). The overall accumulation rate for the period is 0.1 cm/ka, never exceeding 0.3 cm/ka, with pelagic accumulation being an order of magnitude lower. For comparison, Chalk Group accumulation rates average around 2–2.5 cm/ka and may reach 12 cm/ka (Ehrman 1986; Schönfeld et al. 1996; Surlyk et al. 2003). The Cenomanian – late Campanian thus represents 24 Ma characterised by sediment bypass or erosion, with deposition being almost exclusively by mass transport (Fig. 38C).

(c) The overlying 59.4 m thick interval (3411.6–3352.1 m, 11 192 ft 9 in. – 10 997 ft 9 in.) of late Campanian – early Maastrichtian age is a complex succession belonging to FA 2 in which nearly all facies recognised are represented. Pelagic facies
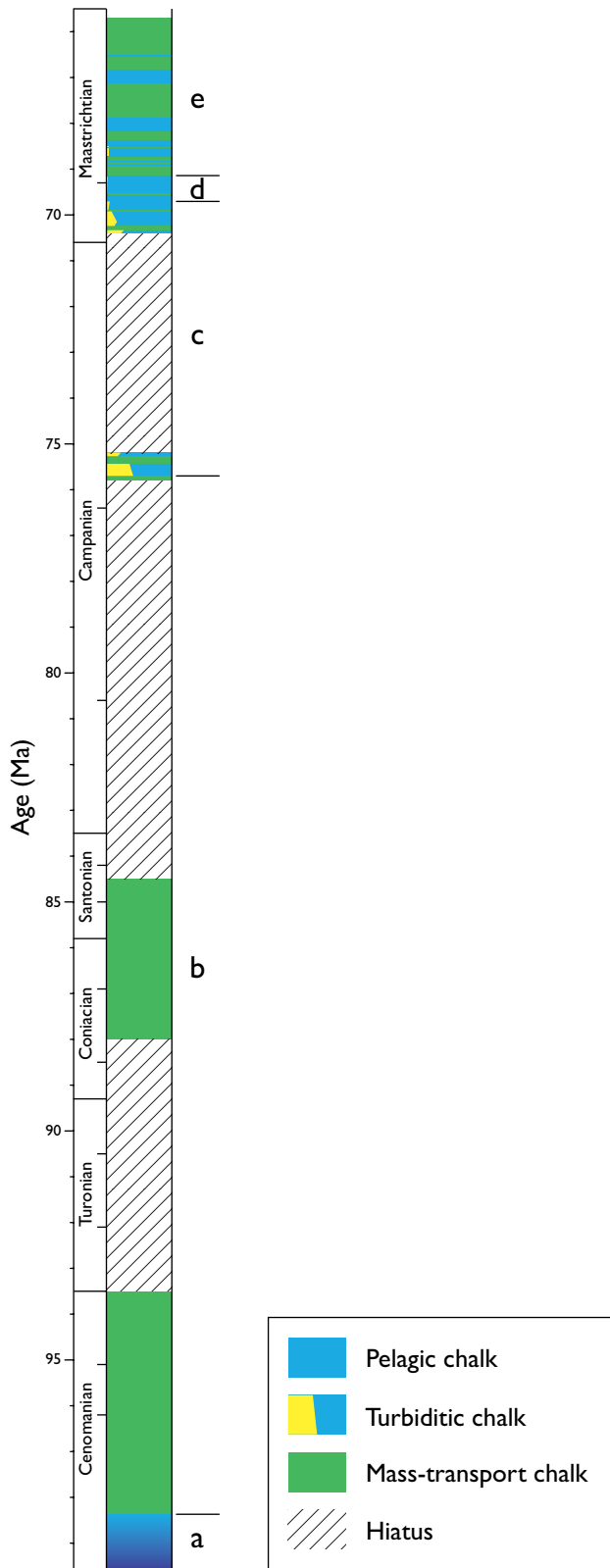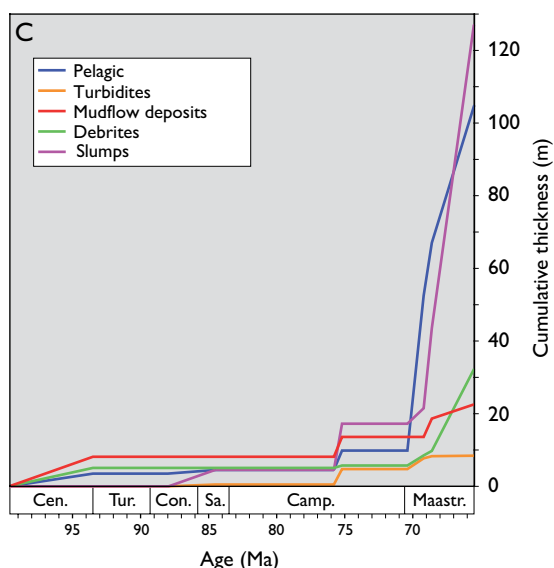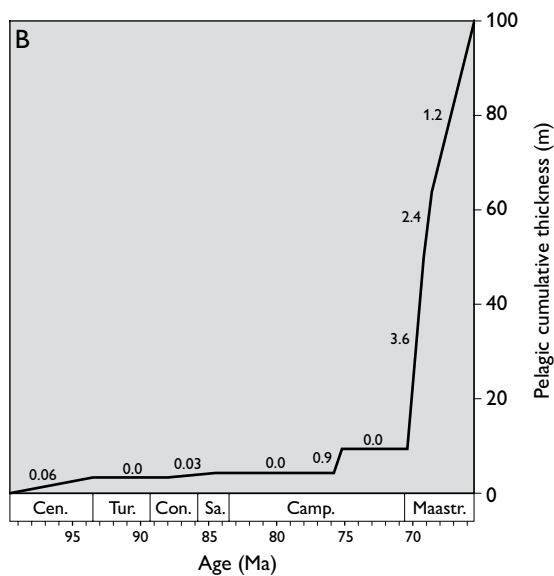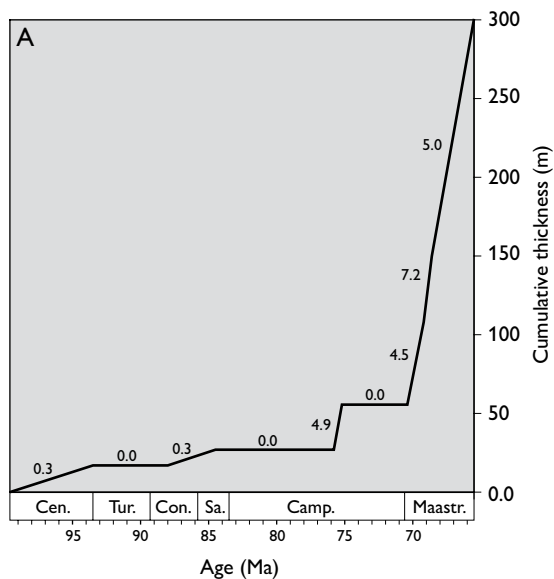
Fig. 37. Simplified log of the studied succession plotted against time. More than half of the Late Cretaceous time interval is represented by hiatuses, and only 10% is represented by pelagites.

are dominated by bioturbated chalk (Facies 1), but laminated chalk (Facies 3) occurs sporadically throughout and dominates the lowermost part, which may be interpreted as a shallowing-upward trend. Turbidites are common to abundant and show a general thinning-upward trend (Fig. 36), which is interpreted to represent gradually decreasing sea-floor topography during progressive basin filling. It should be noted that this interval encompasses a nearly five million-year hiatus according to the available biostratigraphy. Thus, it cannot be determined if the lithological interval represents completely separate depositional systems or a long-term depositional development interrupted by significant erosion. On a smaller scale, sub-intervals showing either thickening- or thinning-upward trends represent prograding or aggrading trends superimposed on the general development. The terms prograding and aggrading are used here to describe the architectural development of the basin-fill, with no implications concerning the position of basin margins or shorelines. There is an upward change in the dominance of the different turbidite facies in the order: Facies 6, 7, 8, and 5, which is interpreted to represent an increase in turbidity flow energy in the lower part of the interval and a gradual decrease in turbidity flow energy in the remainder of the interval (Fig. 34). The stratigraphical development of turbidite facies suggests an initial rapid basinward shift of facies due to prograding basin infill, which represents a short period with a relatively high sedimentation rate (4.9 cm/ka) in the late Campanian. This was followed by five million years with non-deposition or erosion and subsequent gradual shift towards more low-energy turbidite facies and to aggrading basin infill. Intrapelagic erosion surfaces become common in the upper part of the interval.

(d) The overlying 28 m thick interval (3352.1–3324.1 m, 10 997 ft 9 in. – 10 905 ft 10 in.) of early – late Maastrichtian age belongs to FA 1 and is dominated by bioturbated chalk with some intrapelagic erosion surfaces, relatively rare turbidites and thin debrites. This interval is interpreted to represent relatively quiescent tectonic conditions in a low-gradient basin setting.

(e) The remaining 181 m of the studied succession essentially comprises bioturbated chalk and mass-

transport facies of late Maastrichtian age, intervals referred to FA 1 and FA 3. The only exception is a 10.9 m thick interval (3301.7–3290.8 m, 10 832 ft 4 in. – 10 796 ft 6 in.), which belongs to FA 2 and consists of bioturbated chalk, mudflow deposits, thin laminated chalk units, some turbidites and debrites. By far the greater part of the succession accumulated in this period (Fig. 39), when bulk accumulation rates were as high as 7.2 cm/ka, and pelagic accumulation rates were up to 3.6 cm/ka. The late Maastrichtian was thus characterised by relatively quiet pelagic deposition interrupted by large-scale redeposition events. The upward thickening and increasing abundance and dominance of slumps, and probably also debrites, may be due to a progressively shorter distance to the source and deposition further up the flank of the basin margins, or to a gradual increase in the frequency and intensity of triggering events.

The stratigraphic development may thus be summarised as follows: (a) a latest Albian – Cenomanian gradual shift from dominantly hemipelagic, siliciclastic to dominantly pelagic carbonate deposition; (b) a long Cenomanian – late Campanian period associated with tectonic activity and mass transport; (c) late Campanian – early Maastrichtian basin filling dominated by pelagic and turbidite deposition; (d) early – late Maastrichtian basin filling dominated by pelagic deposition; (e) late Maastrichtian basin filling interrupted by increasingly frequent and voluminous mass-transport deposition.

Fig. 38. Cumulative thickness plotted against time for the whole succession (**A**), pelagites (**B**) and genetic units (**C**). Numbers on the curves are accumulation rates in cm/ka. The plots illustrate how most of the succession accumulated during the Maastrichtian, whereas little is preserved from deeper intervals of the Upper Cretaceous. The low accumulation rates during the Cenomanian–Campanian probably reflect the presence of numerous hiatuses below chronostratigraphic resolution. **Cen.**: Cenomanian. **Tur.**: Turonian. **Con.**: Coniacian. **Sa.**: Santonian. **Camp.**: Campanian. **Maastr.**: Maastrichtian.
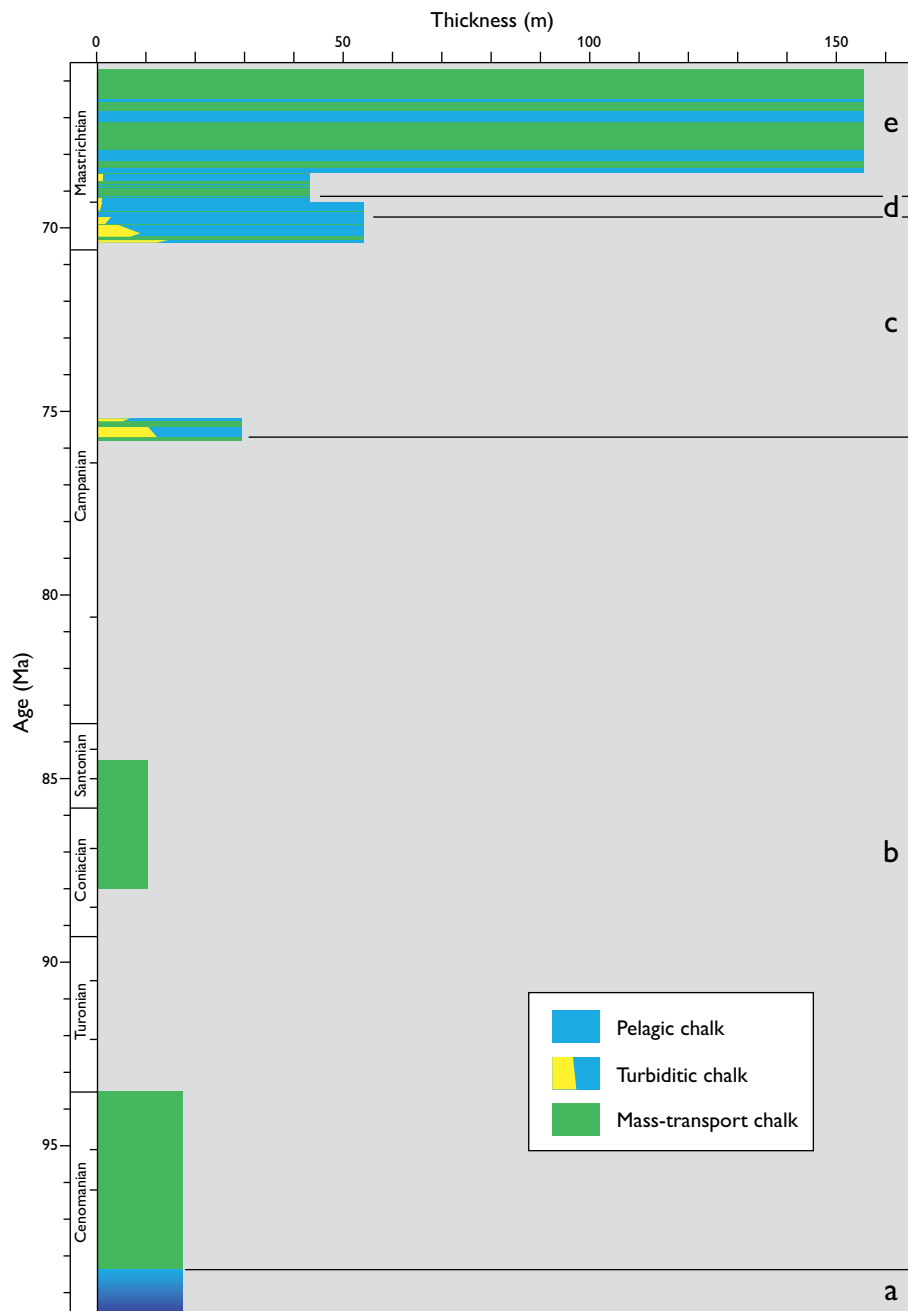
Fig. 39. Simplified log of the studied succession plotted against time and thickness of defined stratigraphic intervals, illustrating the prevalence of Maastrichtian and poor preservation of deeper Upper Cretaceous levels.

Discussion

Basin development and depositional history

The earliest Cenomanian was characterised by the transition from marl to chalk deposition, interrupted by mass-transport events, probably caused by uplift of the Mona Ridge (Figs 40A, 41A) associated with the basin inversion which shifted the local depocentre eastwards from the Jeppe Basin to the Karl Basin (Vejbæk & Andersen 2002). Less than 30 m of sediment, largely mass-transport facies, are preserved in the Cenomanian – upper Campanian succession, indicating that the Mona-1 area was subjected to continuous or pulsed removal of sediments due to uplift of the Mona High and subsidence of the Karl Basin in which deposition was focussed. The Karl Basin was filled during the late Campanian and deposition continued across the Karl Basin, the Mona High area and the Jeppe Basin. During this period, the Mona-1 area was subject to rapid accumulation of pelagic chalk, thin mass-transport chalk, and interbedded turbidites in an overall prograding pattern (Figs 40B, 41B). The absence of the upper Campanian – lower Maastrichtian nannofossil biozone UC17 may indicate erosion due to an inversion pulse (Vejbæk & Andersen 2002) or a significant sea-level drop (Fig. 42) near the Campa-
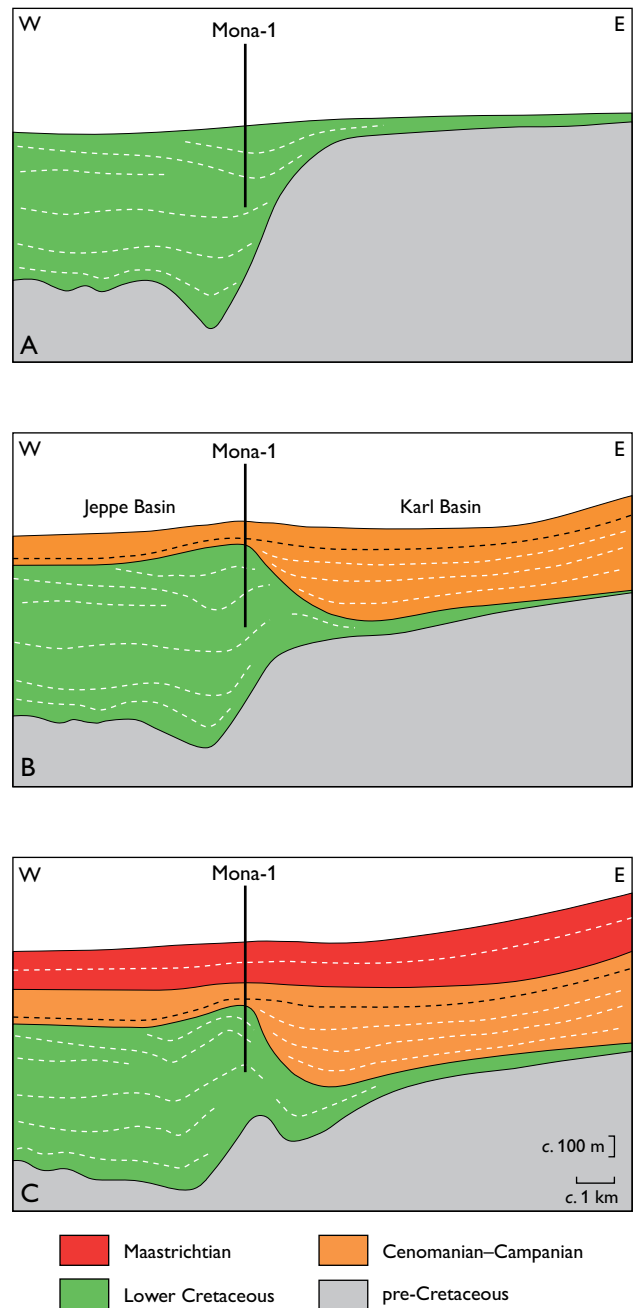
Fig. 40. Interpreted basin evolution based on sedimentological interpretation and seismic section (see Fig. 3). White dashed lines illustrate general reflection patterns, black dashed line represents approximate base of the prograding upper Campanian succession. **A**: Basin configuration in the latest Early Cretaceous, showing the Lower Cretaceous to be largely restricted to the Jeppe Basin. **B**: Basin configuration in the latest Campanian resulting from Cenomanian–Campanian relative uplift of the Mona Ridge and subsidence of the Karl Basin. The dashed black line represents the approximate onset of prograding pelagite/turbidite deposition across the Mona Ridge. Older deposits form a thick succession in the Karl Basin, but are only represented by 30 m of mass-transport deposits and minor pelagites on the Mona Ridge. **C**: Basin configuration in the latest Maastrichtian. The Maastrichtian succession consists of a lower aggrading pelagite/turbidite part and an upper part which is dominated by mass-transport deposits.
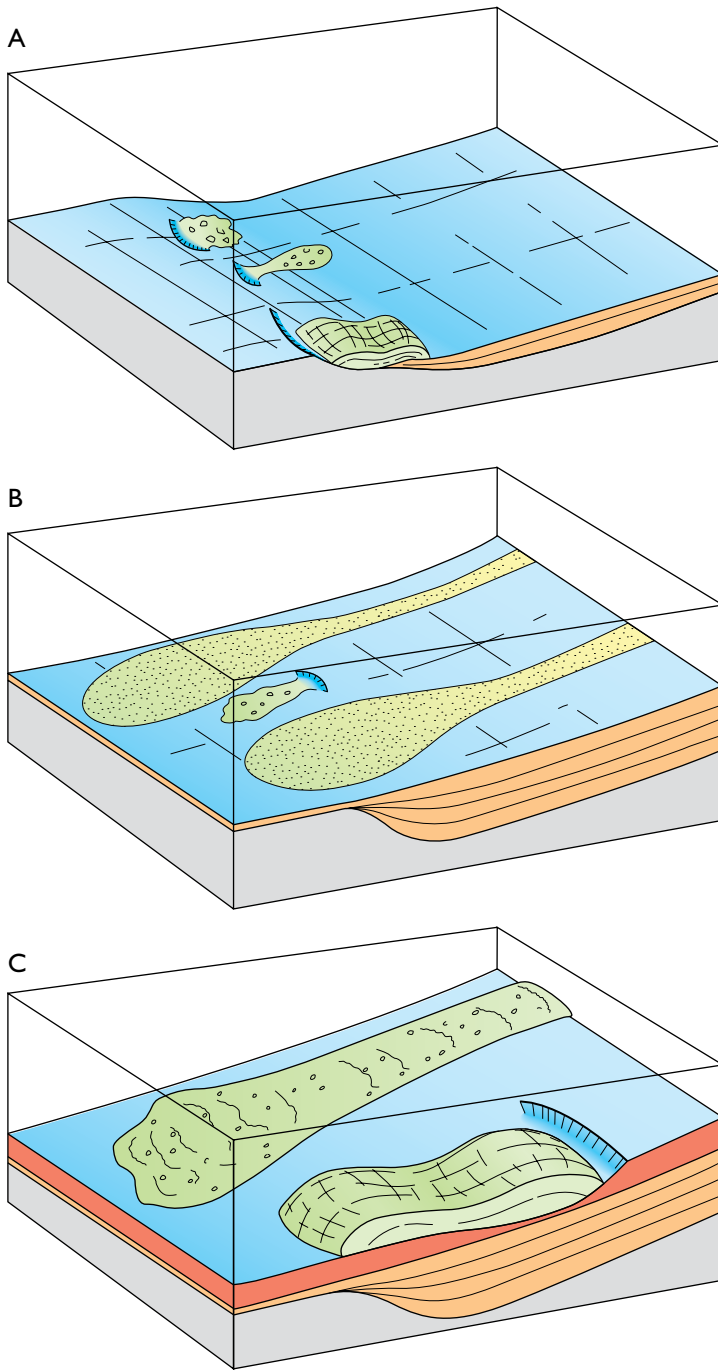
Fig. 41. Interpretation of basin development during the Late Cretaceous in the Mona-1 area. **A**: Cenomanian–Campanian. The Mona-1 area was subjected to continuous or pulsed erosion due to uplift of the Mona Ridge or subsidence in the Karl Basin. Only 30 m of sediment, mainly mass-transport deposits are preserved in Mona-1. The transport direction is speculated to be eastward because Mona-1 is situated slightly eastward, down-slope from the culmination of the Mona Ridge. **B**: Campanian – early Maastrichtian. The Karl Basin was filled and the Mona-1 area was subject to rapid accumulation of a prograding sequence of turbidites and pelagites, perhaps interrupted by an inversion pulse at the Campanian–Maastrichtian boundary. **C**: Late Maastrichtian. Inversion and uplift of the highs east of the Karl Basin caused the depositional environment in the Mona-1 area to be dominated by debris flows and recurrent large-scale slumping.

nian–Maastrichtian boundary. An aggrading pelagic/turbidite succession was deposited at the margin of the Karl Basin at Mona-1 during the early Maastrichtian, followed by pelagic and debris flow deposition with recurrent large-scale slumping during the late Maastrichtian, probably due to inversion and uplift of the highs east of the Karl Basin (Figs 40C, 41C).

It is tempting to link the depositional history to tectonic phases or sea-level variations. Both have probably exerted a major influence on the depositional processes and patterns, but it should be noted that the studied succession is characterised by hiatuses and redeposited units so that almost any postulated sea-level or tectonic event could be roughly correlated to a previously reported event. There are few other wells available in
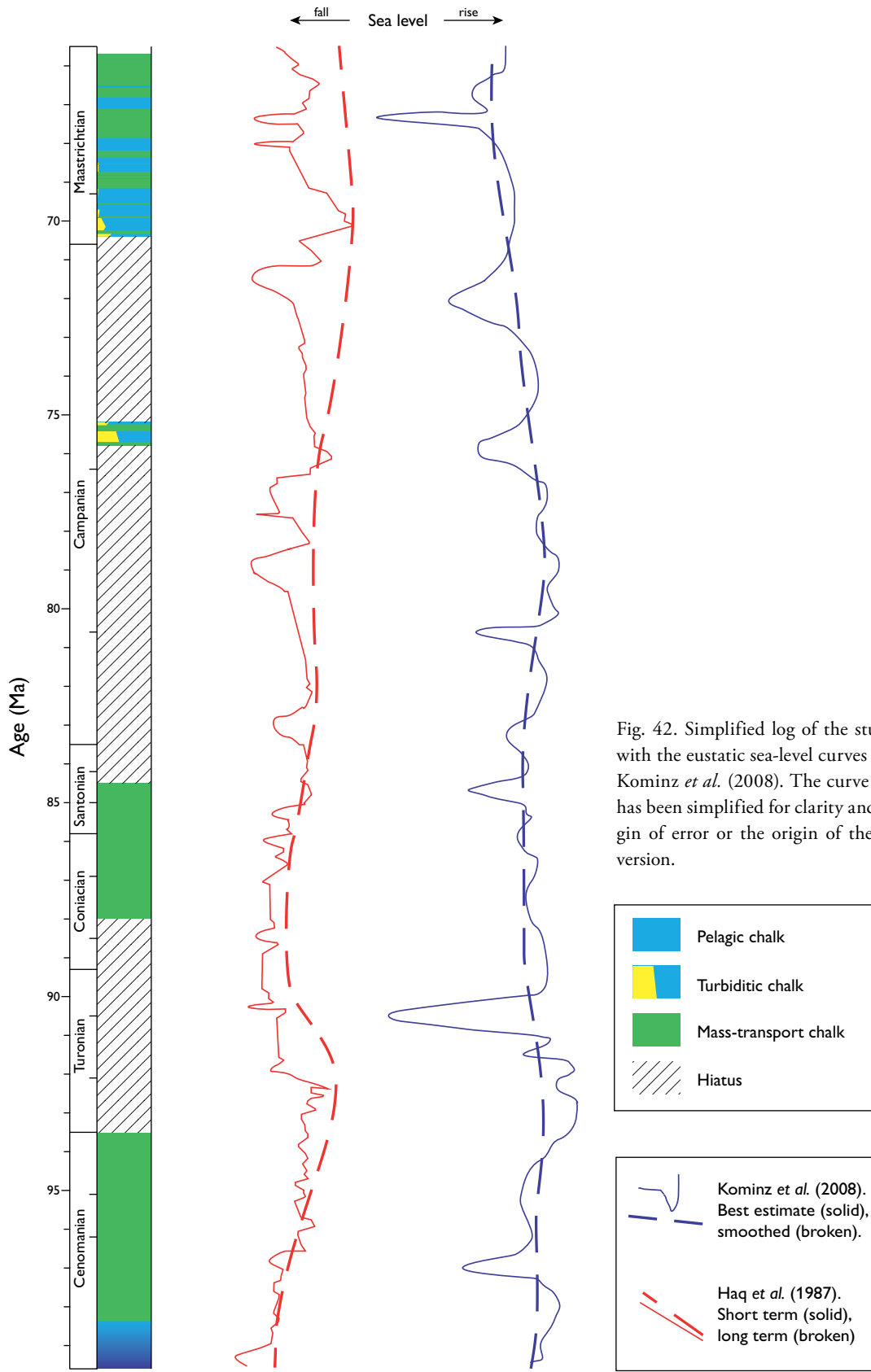
Fig. 42. Simplified log of the studied succession plotted with the eustatic sea-level curves of Haq *et al.* (1987) and Kominz *et al.* (2008). The curve of Kominz *et al.* (2008) has been simplified for clarity and does not show the margin of error or the origin of the data as in the original version.

Pelagic chalk

Turbiditic chalk

Mass-transport chalk

Hiatus

Kominz *et al.* (2008).
Best estimate (solid),
smoothed (broken).

Haq *et al.* (1987).
Short term (solid),
long term (broken)

the study area, and no drill cores covering the Chalk Group. Attempts at linking chalk facies to well-log patterns have yielded rather unconvincing results, which inhibit the correlation of depositional patterns to other wells. Thus, further data and studies are required to place the depositional history of the Mona-1 succession within a regional framework on other than the most general level as outlined above.

Stacking pattern and predictability

Nygaard *et al.* (1983) proposed a model for the spatial and/or temporal evolution of chalk redeposition processes, inspired by Middleton & Hampton (1976). According to the model, flow transformation causes gravity flows to evolve from slide/slump via debris flow and mudflow to turbidity flow. The vertical order of redeposited facies in chalk successions is generally considered chaotic and unpredictable (Surlyk *et al.* 2003), which may have several causes: (1) the redeposition processes are line sourced, (2) the redeposition processes may be initiated at any location on the slope, (3) the dimensions of mass-transport flows are highly variable ranging from small and local to enormous regional-scale events, (4) down-slope flow transformation is highly variable and non-systematic, and (5) different flow conditions may co-exist within a single flow, so that one part of the resulting deposit will be recognised as a slump deposit, whereas another part will be characterised as a debrite. Even if all these causes are valid, there should be a certain probability of encountering particular facies on a particular part of the slope; slumps should thus be more common in the up-slope direction. The Chalk Group in Mona-1 shows a well-defined stacking pattern, although punctuated by numerous hiatuses, comprising a lower basinal succession characterised by a prograding and aggrading turbidite development, overlain by a slope succession dominated by thick slumps and debrites. If similar pat-

terns exist in other chalk settings they may not have been recognised for a number of reasons. Mona-1 is an abnormally long core spanning almost the entire Chalk Group, whereas most cores are much shorter and perhaps cover too little of the succession to detect a subtle upward trend in facies evolution. The turbidites defining the prograding/aggrading pattern constitute volumetrically minor parts of the succession, and the debrites and slumps were most probably line-sourced. Thus, neither turbidites nor mass-transport facies produced geomorphological and bathymetrical elements that were sufficiently dramatic to allow recognition in seismic profiles.

Knowledge about the spatial geometry of the mass-transport complexes is imperative for the further development of a predictive tool. Well logs, principally sonic logs, have been utilised to delineate the distribution of mass-transport complexes in the North Sea chalk (Hatton 1986). The apparent relationship between mass-transport facies and high porosity was extended to the assumption that high-porosity intervals, as revealed by high sonic log values (low velocity), could be taken to represent mass-transport facies, thus involving a certain degree of circular reasoning. This implies that the depositional process is the only or dominant influence on porosity, which is clearly an invalid assumption. Almost all correlations of Hatton (1986) were apparently made between wells with no core control of facies. It was further assumed that high-porosity intervals in wells more than 20 km apart were laterally connected. In other words, if the high-porosity zones did in fact represent mass-transport facies, it was apparently further assumed that they represented the same sedimentary body. Such conclusions thus have far-reaching significance for the understanding of the depositional system, but they may be based on invalid assumptions. Further refinement of geophysical methods and greater integration with sedimentological data are necessary in order to constrain the spatial geometries and connectivity of redeposited chalk bodies.

Conclusions

This analysis of chalk in the exceptionally well-cored Mona-1 borehole has resulted both in the detailed documentation and interpretation of a wide spectrum of facies types and in the elucidation of the depositional evolution of the Mona Ridge area in the Late Cretaceous.

(a) The 303 m thick chalk Upper Cretaceous succession in the Mona-1 core comprises 14 facies representing pelagic deposition, slumping, debris flow, mudflow and turbidity flow.

(b) Pelagic sedimentation probably took place by pelagic fall-out alternating with deposition of thin event beds, and the deposits were thoroughly bioturbated if deposited during periods of full oxygenation of the benthic realm.

(c) Four turbidite facies are recognised and interpreted as having formed by resuspension of unconsolidated chalk ooze on a slope; these different turbidite facies may be related in a high-to-low energy framework.

(d) Clast-supported chalk conglomerates are interpreted to have been directly related to the down-slope evolution of debris flows, which are represented by matrix-supported conglomerates.

(e) Most structureless chalk units were deposited by high-concentration, gravity-driven mudflows, but some burrowed structureless units may have been deposited by rapid fall-out from high-concentration suspension flows.

(f) Limited shear deformation produced distinct quasi-facies from which the precursor facies can be deduced, whereas intense or continued shear deformation produced a shear-banded quasi-facies from which the precursor facies cannot be interpreted in all cases.

(g) More than 40% of the succession was affected by slumping; 14–18 slump events are recognised, and debrites appear to be the most common precursor facies involved in slumping.

(h) The stratigraphic evolution of facies records: (1) a gradual shift from dominantly hemipelagic siliciclastic to dominantly pelagic carbonate deposition in the earliest Cenomanian, interrupted by mass transport and probably uplift of the Mona Ridge; (2) continuous or pulsed erosion and associated mass transport, probably due to uplift of the Mona Ridge, and filling of the Karl Basin during the Cenomanian – late Campanian; (3) pelagic and prograding turbidite basin filling in the late Campanian; (4) probable uplift and erosion of the Mona Ridge close to the Campanian–Maastrichtian boundary; (5) aggrading basin filling dominated by pelagic deposition interrupted by increasingly frequent and voluminous mass-transport deposition during the Maastrichtian.

References

Anderskouv, K., Damholt, T. & Surlyk, F. 2007: Late Maastrichtian chalk mounds, Stevns Klint, Denmark: combined physical and biogenic structures. Sedimentary Geology **200**, 57–72, http://dx.doi.org/10.1016/j.sedgeo.2007.03.005

Bailey, H. *et al.* 1999: A joint chalk stratigraphic framework. Joint Chalk Research Phase V, 203 pp. Stavanger: Norwegian Petroleum Directorate.

Bambach, R.K. 1993: Seafood through time: changes in biomass, energetics, and productivity in the marine ecosystem. Paleobiology **19**, 372–397.

Bouma, A.H. 1962: Sedimentology of some flysch deposits: a graphic approach to facies interpretation, 168 pp. Amsterdam: Elsevier.

Bramwell, N.P., Caillet, G., Meciani, L., Judge, N., Green, M. & Adam, P. 1999: Chalk exploration, the search for a subtle trap. In: Fleet, A.J. & Boldy, S.A.R. (eds): Petroleum geology of Northwest Europe: Proceedings of the 5th Conference. Petroleum Geology Conference Series **5**, 911–937. London: Geological Society.

Brewster, J., Dangerfield, J. & Farrell, H. 1986: The geology and geophysics of the Ekofisk field waterflood. Marine and Petroleum Geology **3**, 139–169, http://dx.doi.org/10.1016/0264-8172(86)90025-5

Britze, P., Japsen, P. & Andersen, C. 1995: Geological map of Denmark 1:200 000. The Danish Central Graben. 'Base Cretaceous' and the Cromer Knoll Gruppen (two-way traveltime and depth, interval velocity and isochore). Danmarks Geologiske Undersøgelse Kortserie **49**, 7 pp., 4 maps.

Burnett, J. 1998: Upper Cretaceous. In: Bown, P.R. (ed.): Calcareous nannofossil biostratigraphy, 132–199. Dordrecht, the Netherlands: Chapman and Hall/Klüwer Academic Publishers.

Cartwright, J.A. 1989: The kinematics of inversion in the Danish Central Graben. In: Cooper, M.A. & Williams, G.D. (eds): Inversion tectonics. Geological Society Special Publications (London) **44**, 153–175.

Crabtree, B. *et al.* (eds) 1996: Description and classification of chalks – North Sea Central Graben. Joint Chalk Research Phase **IV**, 145 pp. Stavanger: Norwegian Petroleum Directorate.

Damholt, T. & Surlyk, F. 2004: Laminated–bioturbated cycles in Maastrichtian chalk of the North Sea: oxygenation fluctuations within the Milankovitch frequency band. Sedimentology **51**, 1323–1342, http://dx.doi.org/10.1111/j.1365-3091.2004.00672.x

Dayton, P.K. & Oliver, J.S. 1977: Antarctic soft-bottom benthos in oligotrophic and eutrophic environments. Science **197**, 55–58, http://dx.doi.org/10.1126/science.197.4298.55

Deegan, C.E. & Scull, B.J. (compilers) 1977: A standard lithostratigraphic nomenclature for the central and northern North Sea. Norwegian Petroleum Directorate (NPD) Bulletin **1**, 36 pp.

Dunham, R.J. 1962: Classification of carbonate rocks according to depositional texture. In: Ham, W.E. (ed.): Classification of carbonate rocks. AAPG Memoirs **1**, 108–121.

Ehrmann, W.U. 1986: Zum Sedimenteintrag in das zentrale nordwesteuropäische Oberkreidemeer. Geologisches Jahrbuch **A97**, 3–139.

Ekdale, A.A. & Bromley, R.G. 1984: Comparative ichnology of shelf-sea and deep-sea chalk. Journal of Paleontology **58**, 322–332.

Embry, A.F. & Klovan, J.E. 1971: A Late Devonian reef tract on northeastern Banks Island, N.W.T. Bulletin of Canadian Petroleum Geology **19**, 730–781.

Esmerode, E.V. & Surlyk, F. 2009: Origin of channel systems in the Upper Cretaceous Chalk Group of the Paris Basin. Marine and Petroleum Geology **26**, 1338–1349.

Esmerode, E.V., Lykke-Andersen, H. & Surlyk, F. 2007: Ridge and valley systems in the Upper Cretaceous chalk of the Danish Basin: contourites in an epeiric sea. In: Viana, A.R. & Rebesco, M. (eds): Economic and palaeoceanographic significance of contourite deposits. Geological Society Special Publications (London) **276**, 265–282.

Esmerode, E.V., Lykke-Andersen, H. & Surlyk, F. 2008: Interaction between bottom currents and slope failure in the Late Cretaceous of the southern Danish Central Graben, North Sea. Journal of the Geological Society (London) **165**, 55–72, http://dx.doi.org/10.1144/0016-76492006-138

Gale, A.S. 1980: Penecontemporaneous folding, sedimentation and erosion in Campanian chalk near Portsmouth, England. Sedimentology **27**, 137–151.

Håkansson, E., Bromley, R. & Perch-Nielsen, K. 1974: Maastrichtian chalk of north-west Europe – a pelagic shelf sediment. In: Hsü, K.J. & Jenkyns, H.C. (eds): Pelagic sediments on land and under the sea. International Association of Sedimentologists Special Publications **1**, 211–233.

Hancock, J. 1975: The sequence of facies in the Upper Cretaceous of northern Europe compared with that in the Western Interior. In: Caldwell, W.G.E. (ed.): The Cretaceous System in the Western Interior of North America. Geological Association of Canada Special Paper **13**, 83–118.

Hancock, J. 1976: The petrology of the chalk. Proceedings of the Geologists' Association **86**, 499–535.

Haq, B.U., Hardenbol, J. & Vail, P.R. 1987: Chronology of fluctuating sea levels since the Triassic. Science **235**, 1156–1167, http://dx.doi.org/10.1126/science.235.4793.1156

Hardman, R.F.P. & Kennedy, W.J. 1980: Chalk reservoirs in the Hod Fields, Norway. Symposium volume 'The sedimentation of the North Sea reservoir rocks', Geilo, May, 1980, Paper **11**, 31 pp. Stavanger: Norwegian Petroleum Society.

Hatton, I.R. 1986: Geometry of allochthonous Chalk Group members, Central Trough, North Sea. Marine and Petroleum Geology **3**, 79–98.

Isaksen, D. & Tonstad, K. 1989 (eds): A revised Cretaceous and Tertiary lithostratigraphic nomenclature for the Norwegian North Sea. Norwegian Petroleum Directorate (NPD) Bulletin **5**, 52 pp.

Johnson, A.M. 1970: Physical processes in geology, 577 pp. San Francisco: Freeman, Cooper & Company.

Kennedy, W.J. 1980: Aspects of chalk sedimentation in the southern Norwegian offshore. Symposium volume 'The sedimentation of the North Sea reservoir rocks', Geilo, May, 1980, Paper **9**, 29 pp. Stavanger: Norwegian Petroleum Society.

Kennedy, W.J. 1987a: Late Cretaceous and Early Palaeocene Chalk Group sedimentation in the Greater Ekofisk area, North Sea Central Graben. Bulletin des Centres de Recherches Exploration-Production Elf-Aquitaine **11**, 91–126.

Kennedy, W.J. 1987b: Sedimentology of Late Cretaceous – Palaeocene chalk reservoirs, North Sea Central Graben. In: Brooks, J. & Glennie, K. (eds): Petroleum geology of North West Europe, 469–481. London: Graham & Trotman.

Kennedy, W.J. & Garrison, R.E., 1975: Morphology and genesis of nodular chalks and hardgrounds in the Upper Cretaceous of southern England. Sedimentology **22**, 311–386, http://dx.doi.org/10.1111/j.1365-3091.1975.tb01637.x

Kennedy, W.J. & Juignet, P. 1974: Carbonate banks and slump beds in Upper Cretaceous (Upper Turonian – Santonian) of Haute Normandie, France. Sedimentology **21**, 1–42, http://dx.doi.org/10.1111/j.1365-3091.1974.tb01780.x

Kominz, M.A., Browning, J.V., Miller, K.G., Sugarman, P.J., Mizintseva, S. & Scotese, C.R. 2008: Late Cretaceous to Miocene sea-level estimates from the New Jersey and Delaware coastal plain coreholes: an error analysis. Basin Research **20**, 211–226, http://dx.doi.org/10.1111/j.1365-2117.2008.00354.x

Krause, F.F. & Oldershaw, A.E. 1979: Submarine carbonate breccia beds – a depositional model for two-layer sediment gravity flows from the Sekwi Formation (Lower Cambrian), Mackenzie Mountains, Northwest Territories, Canada. Canadian Journal of Earth Sciences **16**, 189–199.

Lykke-Andersen, H. & Surlyk, F. 2004: The Cretaceous–Palaeogene boundary at Stevns Klint, Denmark: inversion tectonics or seafloor topography? Journal of the Geological Society (London) **161**, 343–352.

McCave, I.N. 2008: Size sorting during transport and deposition of fine sediments: sortable silt and flow speed. In: Rebesco, M. & Camerlenghi, A. (eds): Contourites. Developments in Sedimentology **60**, 121–142. Amsterdam: Elsevier, http://dx.doi.org/10.1016/S0070-4571(08)10008-5

McKinney, F.K. & Hageman, S.J. 2006: Paleozoic to modern marine ecological shift displayed in the northern Adriatic Sea. Geology **34**, 881–884, http://dx.doi.org/10.1130/G22707.1

Mallon, A.J. & Swarbrick, R.E. 2002: A compaction trend for non-reservoir North Sea Chalk. Marine and Petroleum Geology **19**, 527–539, http://dx.doi.org/10.1016/S0264-8172(02)00027-2

Middleton, G.V. & Hampton, M.A. 1976: Subaqueous sediment transport and deposition by sediment gravity flows. In: Stanley, D.J. & Swift, D.J.P. (eds): Marine sediment transport and environmental management, 197–218. New York: John Wiley & Sons, Inc.

Middleton, G.V. & Wilcock, P.R. 1994: Mechanics in the earth and environmental sciences, 459 pp. Cambridge: Cambridge University Press.

Moscardelli, L. & Woods, L. 2008: New classification system for mass transport complexes in offshore Trinidad. Basin Research **20**, 73–98, http://dx.doi.org/10.1111/j.1365-2117.2007.00340.x

Mullins, H.T. & Cook, H.E. 1986: Carbonate slope apron models: alternatives to the submarine fan model for paleoenvironmental analysis and hydrocarbon exploration. Sedimentary Geology **48**, 37–79, http://dx.doi.org/10.1016/0037-0738(86)90080-1

Nielsen, E.B., Fraselle, G. & Vianello, L. 1990: Tommeliten Gamma Field – Norway Central Graben, North Sea. In: Beaumont, E.A. & Foster, N.H. (eds): Volume **TR**: Structural traps IV: tectonic and nontectonic fold traps, 85–112. AAPG Special Volumes.

Noe-Nygaard, N. & Surlyk, F. 1985: Mound bedding in a sponge-rich Coniacian chalk, Bornholm, Denmark. Bulletin of the Geological Society of Denmark **34**, 237–249.

Nygaard, E., Lieberkind, K. & Frykman, P. 1983: Sedimentology and reservoir parameters of the Chalk Group in the Danish Central Graben. Geologie en Mijnbouw **62**, 177–190.

Ogg, J.G., Agterberg, F.P. & Gradstein, F.M. 2004: The Cretaceous Period. In: Gradstein, F., Ogg, J. & Smith, A. (eds): A geologic time scale 2004, 344–383. Cambridge: Cambridge University Press.

Piper, D.J.W. 1978: Turbidite muds and silts on deep-sea fans and abyssal plains. In: Stanley, D.J. & Kelling, G. (eds): Sedimentation in submarine canyons, fans and trenches, 163–176. Stroudsburg, Pennsylvania: Dowden, Hutchinson & Ross.

Quine, M. & Bosence, D. 1991: Stratal geometries, facies and seafloor erosion in Upper Cretaceous chalk, Normandy, France. Sedimentology **38**, 1113–1152.

Scholle, P.A. 1977: Chalk diagenesis and its relation to petroleum exploration: oil from chalks, a modern miracle? AAPG Bulletin **61**, 982–1009.

Scholle, P.A., Albrechtsen, T. & Tirsgaard, H. 1998: Formation and diagenesis of bedding cycles in uppermost Cretaceous chalks of the Dan Field, Danish North Sea. Sedimentology **45**, 223–243, http://dx.doi.org/10.1046/j.1365-3091.1998.0148e.x

Schönfeld, J. et al. 1996: New results on biostratigraphy, palaeomagnetism, geochemistry and correlation from the standard section for the Upper Cretaceous white chalk of northern Germany (Lägerdorf–Kronsmoor–Hemmoor). Mitteilungen des Geologisch–Paläontologischen Instituts der Universität Hamburg **77**, 545–575.

Siemers, W.T., Caldwell, C.D., Farrel, H.E., Young, C.R., Yang-Logan, J. & Howard, J.J. 1994: Chalk lithofacies, fractures, petrophysics and paleontology: an interactive study of chalk reservoirs. EAPG/AAPG Special Conference on Chalk: Exploration and production from chalk reservoirs, Copenhagen, 7–9 September 1994. Extended abstracts 126–128.

Sikora, P.J., Bergen, J.A. & Farmer, C.L. 1998: Chalk palaeoenvironments and depositional model, Valhall–Hod fields, southern Norwegian North Sea. In: Jones, R.W. & Simmons, M.D. (eds): Biostratigraphy in production and development geology. Geological Society Special Publications (London) **152**, 113–137.

Steinich, G. 1967: Sedimentstrukturen der Rügener Schreibkreide. Geologie **16**, 570–583.

Steinich, G. 1972: Pseudo-Hardgrounds in der Unter-Maastricht-Schreibkreide der Insel Rügen. Wissenschaftliche Zeitschrift der Ernst-Moritz-Arndt-Universität Greifswald, Mathematische-Naturwissenschaftliche Reihe **2**, 213–223.

Stow, D.A.V. & Shanmugam, G. 1980: Sequence of structures in fine-grained turbidites: comparison of recent deep-sea and ancient flysch sediments. Sedimentary Geology **25**, 23–42, http://dx.doi.org/10.1016/0037-0738(80)90052-4

Stow, D.A.V., Reading, H.G. & Collinson, J.D. 1996: Deep seas. In: Reading, H.G. (ed.): Sedimentary environments: processes, facies and stratigraphy, 3rd edition, 395–453. Oxford: Blackwell Science.

Surlyk, F. 1997: A cool-water carbonate ramp with bryozoan mounds: Late Cretaceous – Danian of the Danish Basin. In: James, N.P. & Clarke, J.A.D. (eds): Cool-water carbonates. Society for Sedimentary Geology (SEPM) Special Publication **56**, 293–307.

Surlyk, F. & Lykke-Andersen, H. 2007: Contourite drifts, moats and channels in the Upper Cretaceous chalk of the Danish Basin. Sedimentology **54**, 405–422.

Surlyk, F., Dons, T., Clausen, C.K. & Higham, J. 2003: Upper Cretaceous. In: Evans, D. *et al.* (eds): The Millennium Atlas: petroleum geology of the central and northern North Sea, 213–233. London: Geological Society.

Surlyk, F., Jensen, S.K. & Engkilde, M. 2008: Deep channels in the Cenomanian–Danian Chalk Group of the German North Sea sector: evidence of strong constructional and erosional bottom currents and effect on reservoir quality distribution. AAPG Bulletin **92**, 1565–1586, http://dx.doi.org/10.1306/07100808035

Vejbæk, O.V. & Andersen, C. 2002: Post mid-Cretaceous inversion tectonics in the Danish Central Graben – regionally synchronous tectonic events? Bulletin of the Geological Society of Denmark **49**, 129–144.

Voigt, E. 1962: Frühdiagenetische Deformation der turonen Plänerkalke bei Halle/Westf. als Folge einer Grossgleitung unter besonderer Berücksichtigung des Phacoid-Problems. Mitteilungen aus dem Geologischen Staatsinstitut in Hamburg **31**, 146–275.

Voigt, E. 1977: Neue Daten über die submarine Grossgleitung turoner Gesteine im Teutoburger Wald bei Halle/Westf. Zeitschrift der Deutschen Geologischen Gesellschaft **128**, 57–79.

Voigt, E. & Häntzschel, W. 1964: Gradierte Schichtung in der Oberkreide Westfalens. Fortschritte in der Geologie von Rheinland und Westfalen **7**, 495–548.

Zanella, E. & Coward, M.P. 2003: Structural framework. In: Evans, D. *et al.* (eds): The Millennium Atlas: petroleum geology of the central and northern North Sea, 45–59. London: Geological Society.

Ziegler, P.A. 1990: Geological atlas of western and central Europe, 2nd edition, 239 pp. The Hague: Shell International Petroleum Maatschappij B.V.

De Nationale Geologiske Undersøgelser for Danmark og Grønland (GEUS)

Geological Survey of Denmark and Greenland
Øster Voldgade 10, DK-1350 Copenhagen K, Denmark

The series *Geological Survey of Denmark and Greenland Bulletin* started in 2003 and replaced the two former bulletin series of the Survey, viz. *Geology of Greenland Survey Bulletin* and *Geology of Denmark Survey Bulletin*. Some of the twenty-one volumes published since 1997 in those two series are listed on the facing page. The present series, together with *Geological Survey of Denmark and Greenland Map Series*, now form the peer-reviewed scientific series of the Survey.

Geological Survey of Denmark and Greenland Bulletin

1	The Jurassic of Denmark and Greenland, 948 pp. (28 articles), 2003. *Edited by* J.R. Ineson & F. Surlyk.	500.00
2	Fish otoliths from the Paleocene of Denmark, 94 pp., 2003. *By* W. Schwarzhans.	100.00
3	Late Quaternary environmental changes recorded in the Danish marine molluscan faunas, 268 pp., 2004. *By* K.S. Petersen.	200.00
4	Review of Survey activities 2003, 100 pp. (24 articles), 2004. *Edited by* M. Sønderholm & A.K. Higgins.	180.00
5	The Jurassic of North-East Greenland, 112 pp. (7 articles), 2004. *Edited by* L. Stemmerik & S. Stouge.	160.00
6	East Greenland Caledonides: stratigraphy, structure and geochronology, 93 pp. (6 articles), 2004. *Edited by* A.K. Higgins & F. Kalsbeek.	160.00
7	Review of Survey activities 2004, 80 pp. (19 articles), 2005. *Edited by* M. Sønderholm & A.K. Higgins.	180.00
8	Structural analysis of the Rubjerg Knude Glaciotectonic Complex, Vendsyssel, northern Denmark, 192 pp., 2005. *By* S.A.S. Pedersen.	300.00
9	Scientific results from the deepened Lopra-1 borehole, Faroe Islands, 156 pp. (11 articles), 2006. *Edited by* J.A. Chalmers & R. Waagstein.	240.00
10	Review of Survey activities 2005, 68 pp. (15 articles), 2006. *Edited by* M. Sønderholm & A.K. Higgins.	180.00
11	Precambrian crustal evolution and Cretaceous–Palaeogene faulting in West Greenland, 204 pp. (12 articles), 2006. *Edited by* A.A. Garde & F. Kalsbeek..	240.00
12	Lithostratigraphy of the Palaeogene – Lower Neogene succession of the Danish North Sea, 77 pp., 2007. *By* P. Schiøler, J. Andsbjerg, O.R. Clausen, G. Dam, K. Dybkjær, L. Hamberg, C. Heilmann-Clausen, E.P. Johannessen, L.E. Kristensen, I. Prince & J.A. Rasmussen.	240.00
13	Review of Survey activities 2006, 76 pp. (17 articles), 2007. *Edited by* M. Sønderholm & A.K. Higgins.	180.00
14	Quaternary glaciation history and glaciology of Jakobshavn Isbræ and the Disko Bugt region, West Greenland: a review, 78 pp., 2007. *By* A. Weidick & O. Bennike.	200.00
15	Review of Survey activities 2007, 96 pp. (22 articles), 2008. *Edited by* O. Bennike & A.K. Higgins.	200.00
16	Evaluation of the quality, thermal maturity and distribution of potential source rocks in the Danish part of the Norwegian–Danish Basin, 66 pp., 2008. *By* H.I. Petersen, L.H. Nielsen, J.A. Bojesen-Koefoed, A. Mathiesen, L. Kristensen & F. Dalhoff.	200.00
17	Review of Survey activities 2008, 84 pp. (19 articles), 2009. *Edited by* O. Bennike, A.A. Garde & W.S. Watt.	200.00
18	Greenland from Archaean to Quaternary. Descriptive text to the 1995 Geological map of Greenland, 1:2 500 000. 2nd edition, 126 pp., 2009. *By* N. Henriksen, A.K. Higgins, F. Kalsbeek & T.C.R. Pulvertaft.	280.00
19	Lithostratigraphy of the Cretaceous–Paleocene Nuussuaq Group, Nuussuaq Basin, West Greenland, 171 pp., 2009. *By* G. Dam, G.K. Pedersen, M. Sønderholm, H.H. Midtgaard, L.M. Larsen, H. Nøhr-Hansen & A.K. Pedersen.	300.00
20	Review of Survey activities 2009, 106 pp. (23 articles), 2010. *Edited by* O. Bennike, A.A. Garde & W.S. Watt.	220.00
21	Exploration history and place names of northern East Greenland, 368 pp., 2010. *By* A.K. Higgins.	200.00
22	Lithostratigraphy of the Upper Oligocene – Miocene succession of Denmark, 92 pp., 2010. *By* E.S. Rasmussen, K. Dybkjær & S. Piasecki.	
23	Review of Survey activities 2010, 84 pp. (19 articles), 2011. *Edited by* O. Bennike, A.A. Garde & W.S. Watt.	200.00
24	The East Greenland rifted volcanic margin, 96 pp., 2011. *By* C.K. Brooks.	200.00
25	Upper Cretaceous chalk facies and depositional history recorded in the Mona-1 core, Mona Ridge, Danish North Sea, 60 pp. 2011. *By* K. Anderskouv & F. Surlyk.	200.00

Geological Survey of Denmark and Greenland Map Series

1 Explanatory notes to the Geological map of Greenland, 1:500 000, Humboldt Gletscher, Sheet 6,
48 pp. + map, 2004. *By* P.R. Dawes.   280.00

2 Explanatory notes to the Geological map of Greenland, 1:500 000, Thule, Sheet 5 (1991),
97 pp. + map, 2006. *By* P.R. Dawes.   300.00

3 Explanatory notes to the Geological map of Greenland, 1:100 000, Ussuit 67 V.2 Nord,
40 pp. + map, 2007. *By* J.A.M. van Gool & M. Marker.   280.00

4 Descriptive text to the Geological map of Greenland, 1:500 000, Dove Bugt, Sheet 10,
32 pp. + map, 2009. *By* N. Henriksen & A.K. Higgins   240.00

5 Descriptive text to the Geological map of Greenland, 1:100 000, Kangaatsiaq 68 V.1 Syd and
Ikamiut 68 V.1 Nord, 41 pp. + 2 maps, 2010. *By* A.A. Garde & J.A. Hollis.   280.00

Geology of Greenland Survey Bulletin (discontinued)

181 Precambrian geology of the Disko Bugt region, West Greenland, 179 pp. (15 articles), 1999.
Edited by F. Kalsbeek.   240.00

182 Vertebrate remains from Upper Silurian – Lower Devonian beds of Hall Land, North Greenland,
80 pp., 1999. *By* H. Blom.
120.00

183 Review of Greenland activities 1998, 81 pp. (10 articles), 1999. *Edited by* A.K. Higgins & W.S. Watt.   200.00

184 Collected research papers: palaeontology, geochronology, geochemistry, 62 pp. (6 articles), 1999.   150.00

185 Greenland from Archaean to Quaternary. Descriptive text to the Geological map of Greenland,
1:2 500 000, 93 pp., 2000. *By* N. Henriksen, A.K. Higgins, F. Kalsbeek & T.C.R. Pulvertaft.
Replaced by Geological Survey of Denmark and Greenland Bulletin 18.

186 Review of Greenland activities 1999, 105 pp. (13 articles), 2000. *Edited by* P.R. Dawes & A.K. Higgins.   225.00

187 Palynology and deposition in the Wandel Sea Basin, eastern North Greenland, 101 pp. (6 articles), 2000.
Edited by L. Stemmerik.   160.00

188 The structure of the Cretaceous–Palaeogene sedimentary-volcanic area of Svartenhuk Halvø, central
West Greenland, 40 pp., 2000. *By* J. Gutzon Larsen & T.C.R. Pulvertaft.   130.00

189 Review of Greenland activities 2000, 131 pp. (17 articles), 2001. *Edited by* A.K. Higgins & K. Secher.   160.00

190 The Ilímaussaq alkaline complex, South Greenland: status of mineralogical research with new results,
167 pp. (19 articles), 2001. *Edited by* H. Sørensen.   160.00

191 Review of Greenland activities 2001, 161 pp. (20 articles), 2002. *Edited by* A.K. Higgins, K. Secher &
M. Sønderholm.   200.00

Geology of Denmark Survey Bulletin (discontinued)

36 Petroleum potential and depositional environments of Middle Jurassic coals and non-marine deposits,
Danish Central Graben, with special reference to the Søgne Basin, 78 pp., 1998. *By* H.I. Petersen,
J. Andsbjerg, J.A. Bojesen-Koefoed, H.P. Nytoft & P. Rosenberg.   250.00

37 The Selandian (Paleocene) mollusc fauna from Copenhagen, Denmark: the Poul Harder 1920 collection,
85 pp., 2001. *By* K.I. Schnetler.   150.00

Prices are in Danish kroner exclusive of local taxes, postage and handling

Note that information on the publications of the former Geological Survey of Denmark and the former Geological Survey of Greenland

(amalgamated in 1995 to form the present Geological Survey of Denmark and Greenland) can be found on the Survey's website:

www.geus.dk